PROCEEDINGS OF THE SCHOOL OF ENGINEERING OF TOKAI UNIVERSITY

SERIES E.

VOL. 50, 2025

C O N T E N T S

Technical Papers

Proc. Schl. Eng. Tokai Univ., Ser. E
50 (2025) 1-6
DOI: 10.18995/24343641. 50. 1

Analyses of the Physical Interactions of Human Dolichol Kinase with Other Dolichol-Related Enzymes Involved in the Dolichol Cycle

by

Koki TERAJIMA*1, Tatsuya YAMAMOTO*2, Chinatsu SUGIMURA*2 and Tetsuo TAKAHASHI*3

(Received on Mar. 10, 2025 and accepted on Jun. 20, 2025)

Abstract

In the dolichol cycle which serves to assemble dolichol-linked oligosaccharide (DLO) in the eukaryotic cell, human dolichol kinase (hDK) biosynthesizes dolichol-phosphate (Dol-P), which is in turn utilized by human GlcNAc-1-P transferase (hGPT), Dol-P-mannose synthase (DPMS) complex and Dol-P-glucose synthase (DPGS) as a substrate. In the previous study, we analyzed the membrane topology and physical interaction of hDK using the yeast split-ubiquitin system (YSUS) and revealed that it has at least ten transmembrane domains (TMDs) with both termini oriented toward the cytoplasmic side of the rough ER (rER) membrane and that it physically interacts with itself. In this study, we investigated the physical interactions of hDK with four other human enzymes involved in the dolichol cycle using the YSUS. Our results demonstrated that hDK physically interacted with at least three enzymes (hGPT, hDPM3 and hDPP). In addition, analyses with truncated hDK baits successfully clarified hDK regions required for the interactions with these enzymes.

Keywords: Dolichol kinase, Physical interaction, Split-ubiquitin system

1. Introduction

In eukaryotes the dolichol cycle serves for biosynthesis of dolichol-linked oligosaccharides (DLOs), which is essential for the protein *N*-glycosylation on the rough endoplasmic reticulum (rER) membrane[1]. In the cycle, the dolichol kinase (DK or DOLK) produces dolichyl-phosphate (Dol-P), which directly serves as a scaffold for the assembly of an oligosaccharide portion of DLO on the rER membrane[2-4]. Namely Dol-P is utilized as an acceptor substrate by GlcNAc-1-P transferase (GPT) that is the first enzyme for assembly of DLO. Dol-P is also utilized as an acceptor substrate by dolichyl-phosphate mannose synthase (DPMS) and dolichyl-phosphate glucose synthase (DPGS), which provides donor substrates with luminal mannosyltransferases and glucosyltransferases in the cycle, respectively[1].

We have been investigating the physical interaction of human enzymes involved in dolichol cycle using the yeast split-ubiquitin system (YSUS)[5-8], which has so far identified the physical interaction of various membrane proteins with other membrane proteins[9-14]. Our previous analyses concerning human DK (hDK) by the YSUS revealed that it physically interacted with human GPT (hGPT), hDPM2 and hDPM3 subunits of human DPMS (hDPMS), human DPGS (hDPGS) and human dolichyl-pyrophosphate phosphatase (hDPP) [15-18]. These results were obtained by using hDK as a prey. On the other hand, we have recently carried out experiments using hDK as a bait and successfully demonstrated that it physically interacted with itself[19]. Therefore, in order to verify these interactions between hDK and the four dolichol-related enzymes, we set hDK as a bait of the YSUS and again explored the interactions. Moreover, by preparing novel bait constructs for expressing truncated hDK baits, we tried to refine hDK regions that were required for the interactions with these enzymes.

*1 Graduate Student, Course of Applied Science and Chemistry
*2 Undergraduate Student, Department of Applied Biochemistry
*3 Associate Professor, Department of Bioengineering

2. Experimental Methods

2.1 *Construction of bait recombinant plasmids for the YSUS*

To construct bait recombinant plasmids (bait constructs) for expression of truncated hDK bait proteins, PCR using primers listed in Table 1 was performed as previously described[20], and partial hDK gene was cloned into pBT-N or pBT-C vector by standard cloning method[21),22]. Each truncated hDK bait is illustrated in Fig. 1A. Two bait constructs for expression of full-length hDK (pBT-N-hDK and pBT-C-hDK) have been prepared for previous study.

2.2 *Construction of prey recombinant plasmids for the YSUS*

To construct prey recombinant plasmids (prey constructs)

Table I The PCR primers used in this study. Additional sequences containing a *Sfi* I- cleavage site are shown in lowercase letters.

Primer name	Nucleotide sequence	Purpose
DKBPfw[19]	5'-gtgtaatggccattacggccATGACCCGAGAGTGCCCATCTCCGG-3'	Cloning of *C*-terminally truncated *hDK*
DKBPrv[19]	5'-gcctttggccgaggcggccGCCATCAGCAATATCAGGAGGTAGAG-3'	Cloning of *N*-terminally truncated *hDK*
DK(LR2)BPrv[19]	5'-gcctttggccgaggcggccGTTGCGTGGATGCTCAGCACCA-3'	Cloning of truncated *hDK* from *N*-terminus to LR2
DK(HR2)BPrv	5'-gcctttggccgaggcggcCTTGTATTGGACGTAGAAGGCCTG-3'	Cloning of truncated *hDK* from *N*-terminus to HR2
DK(LR3)BPrv[19]	5'-gcctttggccgaggcggccctGTTTGCGGACATTCGGAACTGG-3'	Cloning of truncated *hDK* from *N*-terminus to LR3
DK(HR3)BPrv	5'-gcctttggccgaggcggcCTGGCACCGCTCCTTCATGACTAGTCCAAG-3'	Cloning of truncated *hDK* from *N*-terminus to HR3
DK(LR4)BPrv[19]	5'-gcctttggccgaggcggccctCTCAAAGAACGGGTTCCCAGCAG-3'	Cloning of truncated *hDK* from *N*-terminus to LR4
DK(HR4)BPrv	5'-gcctttggccgaggcggccAGCGCCAACACTGATGAGAAGAG-3'	Cloning of truncated *hDK* from *N*-terminus to HR4
DK(LR5)BPrv[19]	5'-gcctttggccgaggcggcCACTGGGCGAGTGATGCCGAG-3'	Cloning of truncated *hDK* from *N*-terminus to LR5
DK(*⊿N99*)BPrv	5'-tgtaatggccattacggccatgCAGACTGCTGGGAACCCGTTC-3'	Cloning of truncated *hDK* from LR4 to *C*-terminus
DK(*⊿N109*)BPrv	5'-tgtaatggccattacggccatgTTTGGCATTGTGGTGGCAGCCAC-3'	Cloning of truncated *hDK* from HR4 to *C*-terminus
GBP_fw[17]	5'-tgtaatggccattacggccATGTGGGCCTTCTCGGAATTG-3'	Cloning of full-length *hGPT*
GBP_rv[17]	5'-gcctttggccgaggcggccCAGACATCATAGAAGAGTCGAACG-3'	Cloning of full-length *hGPT*
HsD2BP_fw[16]	5'-tgtaatggccattacggccATGGCCACGGGGACAGACCAGGTG-3'	Cloning of full-length *hDPM2*
HsD2BP_rv[16]	5'-gcctttggccgaggcggcCTGAGCCTTCTTGGTCACTCTCTTGG-3'	Cloning of full-length *hDPM2*
HsD3BP_fw[16]	5'-tgtaatggccattacggccATGACGAAATTAGCGCAGTGGCTTTGG-3'	Cloning of full-length *hDPM3*
HsD3BP_rv[16]	5'-gcctttggccgaggcggccCAGAAGCGCAGCCCCCTGCGGGC-3'	Cloning of full-length *hDPM3*
hA5BPfw[18]	5'-tgtaatggccattacggccATGGCTCCGCTTCTGTTGCAGCTGG-3'	Cloning of full-length *hDPGS*
hA5BPrv[18]	5'-gcctttggccgaggcggccttATTCATTTTCCGAGTTTGCTCAAGCCTC-3'	Cloning of full-length *hDPGS*
DPPBPfw	5'-tgtaatggccattacggccATGGCAGCGGACGGACAGTGCTCG-3'	Cloning of full-length *hDPP*
DPPBPrv	5'-gcctttggccgaggcggcCTGCAGTTTCGTCCCCAGCTTGCG-3'	Cloning of full-length *hDPP*

for expression of prey proteins, PCR using gene-specific primer pairs listed in Table 1 was conducted and full-length hDPP gene was cloned into pPR-N and pPR-C vectors as mentioned above. Prey constructs for other enzymes have been prepared for previous studies. Each full-length prey of hGPT, hDPM2, hDPM3, hDPGS and hDPP is also illustrated in Fig. 1B.

2.3 *Assays for the physical interaction*

Each of the bait constructs for hDK, which was showed in Fig. 1A, was combined with each of the prey constructs for hGPT, hDPM2, hDPM3, hDPGS and hDPP, which was showed in Fig. 1B, and then they were used for co-transformation[23] of yeast NMY51 strain. After the co-transformation, the co-transformants grown on SD-LW medium were subject to growth examination with SD-LWH and SD-LWHA media, according to the same procedure as previously described[19]. Co-transformants of each bait construct with the negative or positive control prey construct (pDL-Alg5 or pAI-Alg5, respectively) were always used on growth examinations in this study.

3. Results and Discussion

3.1 *The physical interaction of full-length hDK with the three enzymes*

Growth tests using the full-length hDK bait (pBT-N-hDK) showed that hDK could interact with the *N*-terminally tagged preys of hGPT, hDPM3 and hDPP (left side in Fig. 2). In contrast, the same bait did not show interaction with hDPM2 or hDPGS. Furthermore, no interaction was detected between this hDK bait and the *C*-terminally tagged preys of all enzymes tested. These findings suggest that the *N*-terminus of hDK is positioned close to the *N*-termini of the three interacting proteins (hGPT, hDPM3 and hDPP), and distant from the *C*-termini of the

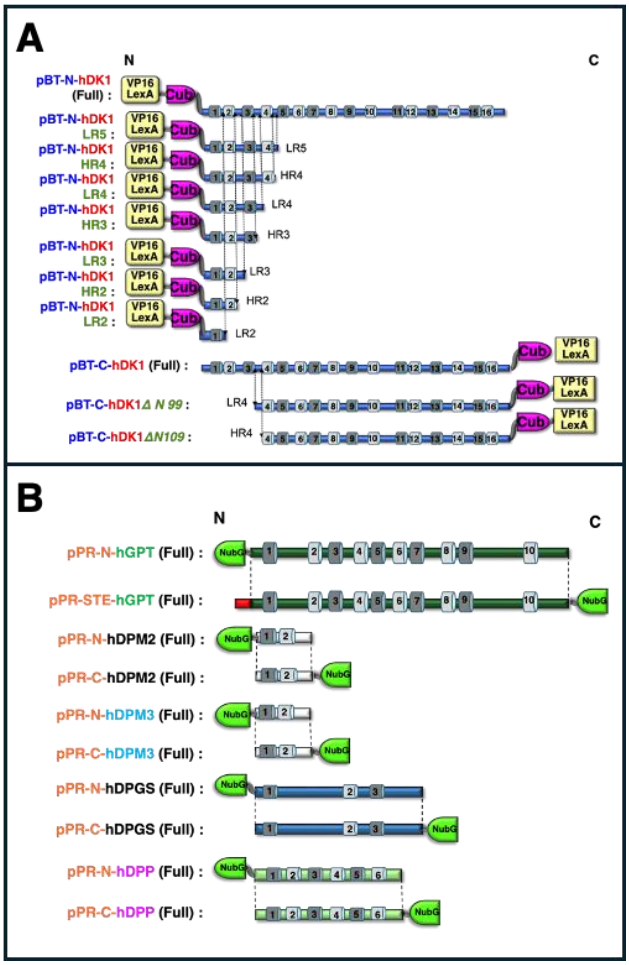

Fig. 1 Plasmid constructs and expressed proteins in this study. Bars and boxes of proteins indicate loop regions (LRs) and hydrophobic regions (HRs), respectively. A; bait constructs for full-length and truncated hDKs. B; prey constructs for full-length hGPT, hDPM2, hDPM3, hDPGS and hDPP. Red stretch indicates STE sequence added for protein stabilization.

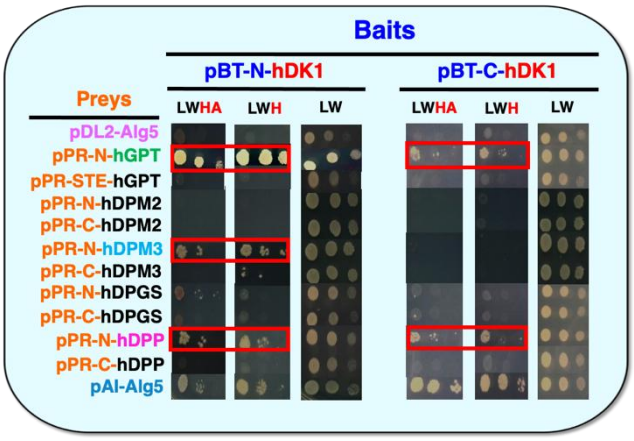

Fig. 2 Growth examination of co-transformants using two full-length hDK baits. After the selection of colonies derived from the co-transformants on the SD-LW medium, their suspensions were diluted with sterilized water and adjusted to the OD_{600} values of 1.0, 0.1 and 0.01 (from left to right). These diluents were orderly spotted on the SD-LWH and SD-LWHA media for reporter detection, and SD-LW media for growth control, and then incubated at 30 ºC for 2~4 days.

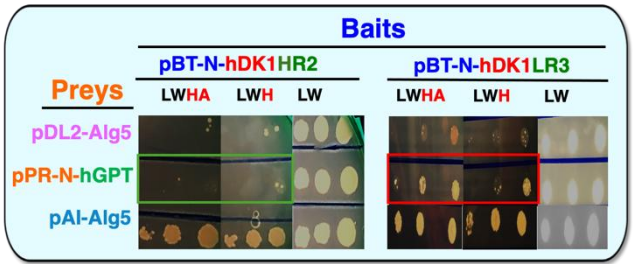

Fig. 3 Growth examination of co-transformants using truncated hDK baits and full-length hGPT prey. The experiments were carried out according to the same procedure as described in the legend of Fig. 2, except reverse order of spotting.

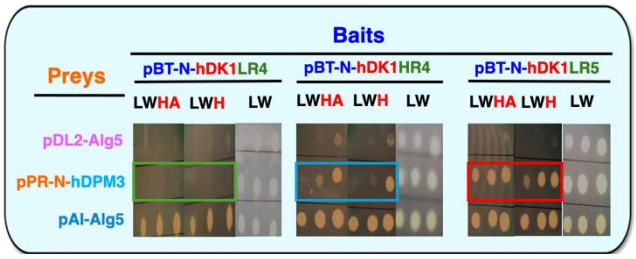

Fig. 4 Growth examination of co-transformants using truncated hDK baits and full-length hDPM3 prey. The experiments were carried out according to the same procedure as described in the legend of Fig. 3.

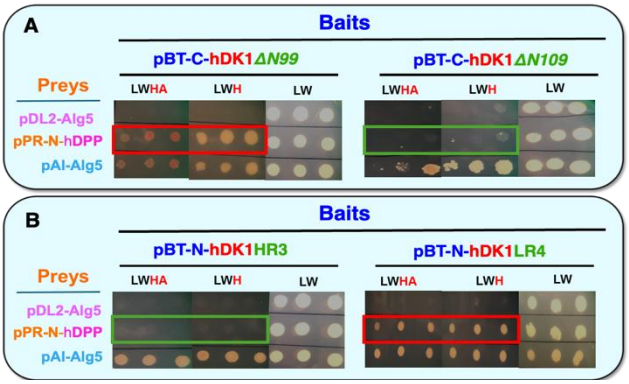

Fig. 5 Growth examination of co-transformants using truncated hDK baits and full-length hDPP prey. The experiments were carried out according to the same procedure as described in the legend of Fig. 3.

tested proteins.

Similar results were obtained using the *C*-terminally tagged hDK bait (pBT-C-hDK), except for a difference with the *N*-terminally tagged hDPM3 prey (right side in Fig. 2). Because of this, we selected the *N*-terminally tagged hDK for further analyses of interactions with hGPT, hDPM3 and hDPP.

3.2 *The physical interaction of truncated hDK with hGPT*

To identify the region of hDK responsible for binding to hGPT, we tested seven newly prepared truncated hDK baits (Fig. 1A, upper). Growth assays revealed that co-transformants with pBT-N-hDK/LR5, pBT-N-hDK/HR4, pBT-N-hDK/LR4 and pBT-N-hDK/HR3 showed growth on selective media,

similar to the full-length construct. The pBT-N-hDK/LR3 bait also supported growth, indicating that truncations up to LR3 still maintained interaction with hGPT (Fig. 3, red frame). However, the pBT-N-hDK/HR2 construct, which lacks LR3, failed to support growth (Fig. 3, green frame). These observations clearly show that the LR3 region of hDK is critical for its interaction with hGPT, while the region from HR3 to the *C*-terminus is not essential.

3.3 *The physical interaction of truncated hDK with hDPM3*

When truncated hDK baits were tested for interaction with hDPM3, the pBT-N-hDK/LR5 construct supported growth on selective media, similar to the full-length hDK bait (Fig. 4, red frame). However, the pBT-N-hDK/HR4 construct, which lacks LR5, showed reduced growth (Fig. 4, blue frame). Furthermore, the pBT-N-hDK/LR4 construct, which lacks both LR5 and HR4, showed no growth at all (Fig. 4, green frame). These results suggest that both HR4 and LR5 regions of hDK are necessary for stable interaction with hDPM3.

3.4 *The physical interaction of truncated hDK with hDPP*

Growth tests of truncated hDK baits with hDPP showed that the LR4 region is essential for this interaction. The pBT-N-hDK/LR4 construct retained normal growth, similar to the full-length bait (Fig. 5B, red frame). However, the pBT-N-hDK/HR3 construct, which lacks LR4, showed no growth (Fig. 5B, green frame). These results indicate that LR4 is required for hDK-hDPP binding.

We further tested *N*-terminally truncated hDK constructs (Fig. 1A, lower). The pBT-C-hDK*ΔN99* construct, which lacks the region from the *N*-terminus to HR3, still interacted with hDPP (Fig. 5A, red frame). In contrast, the pBT-C-hDK*ΔN109* construct, which lacks the region from the *N*-terminus to LR4, showed no interaction (Fig. 5B, green frame). These additional results strongly support the conclusion that LR4 is essential for the interaction between hDK and hDPP.

4. Conclusion

In our previous work, we used hGPT, two subunits of hDPMS (hDPM2 and hDPM3), hDPGS and hDPP as baits and detected their physical interactions with hDK prey[15-18]. In order to confirm and extend these findings, in this study we tested hDK as bait and examined its interactions with the same four Dol-P-related enzymes in the dolichol cycle using the yeast split-ubiquitin system. Through this analysis, we were able to reconfirm three interactions of hDK: with hGPT, hDPM3, and hDPP. However, no interactions were detected with hDPM2 or hDPGS, and the reason for this remains unknown.

To explore the binding regions of hDK, we prepared several truncated hDK baits and examined their interactions. Our results revealed that LR3 of hDK is required for interaction with hGPT, while LR4 is required for interaction with hDPP. In addition, both HR4 and LR5 were shown to contribute to the interaction with hDPM3. Taken together, these results demonstrate that hDK interacts with different

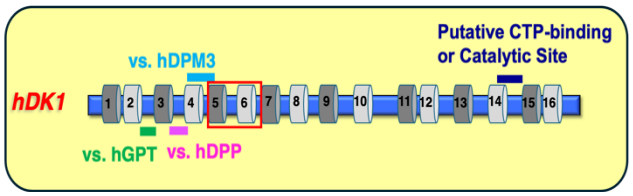

Fig. 6 Summary of interacting regions of hDK. A red frame indicates a region that are critical of self-interaction of hDK[19]. Refinement of hDK regions for the physical interactions with hGPT, hDPM3 and hDPP is based on the results of Fig. 3, Fig. 4 and Fig. 5, respectively.

enzymes through distinct regions. Interestingly, these regions are all located in the *N*-terminal half of hDK, whereas the catalytic site of hDK is known to be close to the *C*-terminus. This suggests that the *N*-terminal regions of hDK, including LR3, LR4, HR4, and LR5, may have a regulatory role, possibly controlling the enzymatic activity of hDK through allosteric effects.

In our recent work, we also identified another important region, HR5-LR7, that is essential for hDK self-interaction. Thus, it appears that multiple functional regions in the *N*-terminal half of hDK mediate interactions not only with other enzymes but also with hDK itself. Considering the overall structural arrangement, it is likely that hDK activity and stability are controlled by a complex network of protein-protein interactions. With rapid advances in structural biology, predictions of membrane protein conformations have become increasingly accurate. It is expected that in the near future, the detailed structures of protein complexes on membranes, such as those involving hDK, will be predicted or experimentally determined. Our results from the YSUS analysis will provide important information for future studies aiming to elucidate the quaternary structure and stoichiometry of hDK.

It is also important to note that mutations or deficiencies in hDK cause severe congenital disorders of glycosylation, known as CDG-Im, DK1-CDG, or DOLK-CDG[24-31]. Even when hDK retains normal enzymatic activity, abnormality in its physical interactions may lead to defects in DLO assembly and consequently impair *N*-glycosylation. Therefore, our findings on the physical interactions of hDK are significant, as they may help to evaluate the functional effectiveness of hDK in both normal and disease states.

References

1) M. Aebi, *N*-linked protein glycosylation in the ER, Biochim. Biophys. Acta Vol.1833, pp.2430-2437 (2013).
2) M. Bernstein, F. Kepes and R. Schekman, *SEC59* encodes a membrane protein required for core glycosylation in *Saccharomyces cerevisiae*, Mol. Cell. Biol. Vol.9, pp.1191-1199 (1989).
3) L. Heller, P. Orlean and W. L. Adair Jr., *Saccharomyces cerevisiae* sec59 cells are deficient in dolichol kinase activity, Proc. Natl. Acad. Sci. USA Vol.89, pp.7013-7016 (1992).
4) F. Fernandez, P. Shridas, S. Jiang, M. Aebi, C. J. Waechter, Expression and characterization of a human

cDNA that complements the temperature-sensitive defect in dolichol kinase activity in the yeast *sec59-1* mutant: the enzymatic phosphorylation of dolichol and diacylglycerol are catalyzed by separate CTP-mediated kinase activities in *Saccharomyces cerevisiae*. Glycobiology Vol.12, pp.555–562 (2002).

5) N. Johnsson and A. Varshavsky, Split ubiquitin as a sensor of protein interactions *in vivo*, Proc. Natl. Acad. Sci. USA Vol.91, No.22, pp.10340-10344 (1994).
6) I. Stagljar, C. Korostensky, N. Johnsson and S. te Heesen, A genetic system based on split-ubiquitin for the analysis of interactions between membrane proteins *in vivo*, Proc. Natl. Acad. Sci. USA Vol.95, pp.5187-5192 (1998).
7) M. Fetchko and I. Stagljar, Application of the split-ubiquitin membrane yeast two-hybrid system to investigate membrane protein interactions, Methods Vol.32, pp.349-362 (2004).
8) S. Thaminy, J. Miller and I. Stagljar, The split-ubiquitin membrane-based yeast two-hybrid system, Methods. Mol. Biol. Vol.261, pp.297–312 (2004).
9) M. Dünnwald, A. Varshavsky and N. Johnsson, Detection of transient *in vivo* interaction between substrate and transporter during protein translocation into the endoplasmic reticulum, Mol. Biol. Cell Vol.10, pp.329-344 (1999).
10) M. J. Massaad and A. Herscovics, Interaction of the endoplasmic reticulum alpha 1,2-mannosidase Mns1p with Rer1p using the split-ubiquitin system. J. Cell Sci. Vol.114, pp.4629-4635 (2001).
11) W. Scheper, S. Thaminy, S. Kais, I. Stagljar and K. Römisch, Coordination of *N*-glycosylation and protein translocation across the endoplasmic reticulum membrane by Sss1 protein, J. Biol. Chem. Vol.278, No.39, pp.37998-38003 (2003).
12) A. Yan and W. J. Lennarz, Studies on yeast oligosaccharyl transferase subunits using the split-ubiquitin system: Topological features and *in vivo* interactions, Proc. Natl. Acad. Sci. USA Vol.102, No.20, pp.7121-7126 (2005).
13) T. Takahashi and T. Takeuchi, Membrane topological characterization of the human Alg14 protein, Proc. Schl. Eng. Tokai Univ., Ser. E Vol.44, pp.1-6 (2019).
14) Samantha and T. Takahashi, Analyses of the membrane topology and physical interaction of dolichyl-phosphate-glucose synthase Alg5p, Proc. Schl. Eng. Tokai Univ., Ser. E Vol.49, pp.19-25 (2024).
15) T. Takahashi and X. -D. Gao, Physical interactions among human glycosyltransferases involved in dolichol-linked oligosaccharide biosynthesis, Trends in Glycoscience and Glycotechnology Vol.24, No.136, pp.65-77 (2012).
16) T. Takahashi, N. Yamada and N. Kurimoto, Analyses on the physical interactions of the human dolichyl-phosphate-mannose synthase, Proc. Schl. Eng. Tokai Univ., Ser. J. Vol.57, No.1, pp.5-10 (2017).
17) T. Takahashi, K. Nishimura, N. Maeda and R. Oshiro, Characterization of the membrane topology and physical interaction of human *N*-acetylglucosamine-1-phosphate transferase, Proc. Schl. Eng. Tokai Univ., Ser. E Vol.46, pp.1-6 (2021).
18) T. Takahashi, N. Yamada and R. Oshiro, Characterization of the membrane topology and physical interaction of human dolichol-phosphate-glucose synthase, Proc. Schl. Eng. Tokai Univ., Ser. E Vol.47, pp.1-6 (2022).
19) T. Takahashi, E. Horigome, T. Yamanoto and K. Terajima, Analyses of the membrane topology and physical interaction of human dolichol kinase, Proc. Schl. Eng. Tokai Univ., Ser. E Vol.49, pp.13-18 (2024).
20) H. A. Erlich, PCR Technology, Stockton Press, pp.61-70 (1989).
21) H. Inoue, H. Nojima and H. Okayama, High efficiency transformation of *Escherichia coli* with plasmids, Gene Vol. 96, pp.23–28 (1990).
22) L. Sambrook, E. F. Fritsch and T. Maniatis, Molecular Cloning: A Laboratory Manual. Second edition, Cold Spring Harbor Laboratory Press, NY, (1989).
23) H. Ito, Y. Fukuda, K. Murata and A. Kimura, Transformation of intact yeast cells treated with alkali cations, J. Bacteriol. Vol.153, No.1, pp.163-168 (1983).
24) C. Kanz, C. Jungeblut, J. Denecke, A. Erlekotte, C. Sohlbach, V. Debus, H. G. Kehl, E. Harms, A. Reith, S. Reichel, H. Gröbe, G. Hammersen, U. Schwarzer and T. Marquardt, A defect in dolichol phosphate biosynthesis causes a new inherited disorder with death in early infancy, Amer. J. Hum. Genet. Vol.80, No.3, pp.433-440 (2007).
25) D. J. Lefeber, A. P. de Brouwer, E. Morava, M. Riemersma, J. H. Schuurs-Hoeijmakers, B. Absmanner, K. Verrijp, W. M. van den Akker, K. Huijben, G. Steenbergen, J. van Reeuwijk, A. Jozwiak, N. Zucker,A. Lorber, M. Lammens, C. Knopf, H. van Bokhoven, S. Grünewald, L. Lehle, L. Kapusta, H. Mandel and R. A. Wevers, Autosomal recessive dilated cardiomyopathy due to DOLK mutations results from abnormal dystroglycan *O*-mannosylation, PLOS Genet. Vol.7, No.12, e1002427, doi: 10.1371/journal.pgen.1002427 (2011).
26) L. Kapusta L, N. Zucker, G. Frenckel, B. Medalion, T. Ben Gal, E. Brik, H. Mandel, N. Nasser, S. Morgenstern, A. Zuckermann, D. J. Lefeber, A. de Brouwer, R. A. Wevers, A. Lorber and E. Morava, From discrete dilated cardiomyopathy to successful cardiac transplantation in congenital disorders of glycosylation due to dolichol kinase deficiency (DK1-CDG), Heart Fail. Rev. Vol.18, No.2, pp.187-196 (2013).
27) A. Helander, T. Stödberg, J. Jaeken, G. Matthijs, M. Eriksson and G. Eggertsen, Dolichol kinase deficiency (DOLK-CDG) with a purely neurological presentation caused by a novel mutation, Mol. Genet. Metab. Vol.110, No.3, pp.342-344 (2013).
28) M. T. Lieu, B. G. Ng, J. S. Rush, T. Wood, M. J. Basehore, M. Hegde, R. C. Chang, J. E. Abdenur, H. H. Freeze and R. Y. Wang, Severe, fatal multisystem manifestations in a patient with dolichol kinase-

congenital disorder of glycosylation, Mol. Genet. Metab. Vol.110, No.4, pp.484-489 (2013).
29) E. T. Rush, C. V. Baker and W. B. Rizzo, Dolichol kinase deficiency (DOLK-CDG): two new cases and expansion of phenotype, Amer. J. Med. Genet. Part A, Vol.173, No.39, pp.2428-2434 (2017).
30) K. Komiosi, O. Claris, S. Collardeau-Frachon, J. Kopp, I. Hausser, J. Mazereeuw-Hautier, N. Jonca, A. D. Zimmer, D. Sanlaville and J. Fischer, Fatal neonatal DOLK-CDG as a rare form of syndromic ichthyosis, Front. Genet. Vol.12, 719624, doi: 10.3389/fgene.2021.719624 (2021).
31) S. Yu, Y. Zhang, Z. Chen, J. Song and C. Wang, A novel compound heterozygous gene mutation of dolichol kinase deficiency (DOLK-CDG), Endocr. Metab. Immune Disord. Drug. Targets Vol.23 No.2, pp.235-241 (2023).

Proc. Schl. Eng. Tokai Univ., Ser. E
50 (2025) 7-11
DOI: 10.18995/24343641. 50. 7

Analyses of the Physical Interactions of Yeast Alg5p with Dolichyl-Phosphate-Related Enzymes in the Dolichol Cycle

by

SAMANTHA[*1], Nanami ADACHI[*2] and Tetsuo TAKAHASHI[*3]

(Received on Mar. 17, 2025 and accepted on Jun. 20, 2025)

Abstract

In the dolichol cycle for assembling dolichol-linked oligosaccharide (DLO), yeast dolichyl-phosphate-glucose synthase (DPGS), Alg5p, produces dolichyl-phosphate-glucose (DPG). Previously we investigated the physical interaction of Alg5p and demonstrated that it physically interacts with Dpm1p, Sec59p, Cwh8p and Alg7p, all of which are involved in the dolichol cycle. In this study, we further investigated the physical interactions of Alg5p with Dpm1p, Sec59p and Cwh8p in detail and successfully refined regions essential for each interaction on Alg5p. Our results strongly suggest that the physical interactions of Alg5p might occur on both *N*- and *C*-terminal portions. Namely, it was considered that the *N*-terminal portion of Alg5 is crucial for the interaction with Dpm1p, while the *C*-terminal portion is critical for the interaction with Sec59p and Cwh8p in addition to Alg7p and Alg5p itself.

Keywords: Dolichyl-phosphate-glucose synthase, Physical interaction, Split-ubiquitin system

1. Introduction

The assembly of dolichol-linked oligosaccharides (DLOs) on the rough endoplasmic reticulum (rER) membrane is conducted by a biosynthetic pathway known as dolichol cycle, which is essential for the protein *N*-glycosylation in yeast[1-5]. In the cycle, dolichyl-phosphate-glucose (DPG) is required for three luminal glucosyltransferases (Alg6p, Alg8p and Alg10p) as a donor substrate, and provided by DPG synthase (DPGS)[6]. Yeast Alg5p protein is the DPGS that was firstly identified and characterized in eukaryotes[7][8].

The yeast split-ubiquitin system (YSUS) is a technique which was specially devised for detection of physical interaction between two membrane proteins[9-12]. By using the YSUS, many interactions of membrane proteins have been successfully uncovered so far[13-21]. By using it, we have previously investigated the membrane topology of Alg5p and demonstrated that it had two transmembrane domains with both termini oriented toward the cytoplasmic side of the rER membrane[22),23]. We also investigated the physical interaction of Alg5p and detected its interaction with itself and four dolichyl-phosphate (Dol-P)-related enzymes (Dpm1p, Sec59p, Cwh8p and Alg7p) in the dolichol cycle[22),23]. Dpm1p is dolichyl-phosphate-mannose (DPM) synthase (DPMS), which shares Dol-P with Alg5p as an acceptor substrate[24)25]. Alg7p is GlcNAc-1-P transferase (GPT), which also utilizes Dol-P as an acceptor substrate[26]. Sec59p is dolichol kinase (DK), which *de novo* produces Dol-P[27]. Cwh8p is dolichyl-pyrophosphate phosphatase (DPP), which also produces Dol-P[28),29]. In addition, we refined the regions which are required for the self-interaction of Alg5p and interaction with Alg7p by using several truncated Alg5p baits in the previous reserach[22),23]. Therefore, using novel truncated baits additionally, we also tried to refine regions on Alg5p, which are important for the interactions with Dpm1p, Sec59p and Cwh8p.

*1 Graduate Student, Course of Applied Science and Chemistry
*2 Undergraduate Student, Department of Bioengineering
*3 Associate Professor, Department of Bioengineering

2. Experimental Methods

2.1 *Construction of recombinant plasmids for expression of truncated Alg5p baits*

In our previous study, we prepared five bait recombinant plasmids (bait constructs) for expression of truncated Alg5p[23]. One of them, pBT-C-ALG5HR2 was again used in this study (Fig. 1). In addition, six novel bait constructs were prepared as follows. PCRs were performed using forward primer AG5_fw and each of reverse primers (AG5HR1_rv, AG5LR2_rv, AG5HR2_rv and AG5LR3_rv) by standard method[30] and then amplified DNA fragments were cloned into the pBT-N vector to generate pBT-N-ALG5HR1, pBT-N-ALG5LR2, pBT-N-ALG5HR2 and pBT-N-ALG5LR2, respectively (Fig. 1). In addition, PCRs were performed using forward primer (AG5*ΔN10*_BPfw or AG5*ΔN10*_BPf) and reverse primer AG5_rv by standard method[30] and then amplified DNA fragments were cloned into the pBT-C vector to generate pBT-C-ALG5*ΔN10* and pBT-C-ALG5*ΔN33* bait constructs, respectively (Fig. 1). PCR primers are listed in Table 1 and DNA cloning was conducted according to the same procedure as previously described[31),32].

Table I The PCR primers used in this study. Additional sequences containing a *Sfi* I- cleavage site are shown in lowercase letters.

Primer name	Nucleotide sequence	Purpose
AG5_fw[22]	5'-tgtaatggccattacggccATGAGAGCGTTGAGATTCCTGATTG-3'	Cloning of *C*-terminally truncated *ALG5*
AG5_rv[22]	5'-gcctttggccgaggcggccCATTTCTTATTATCTCTATATATCCCTAA-3'	Cloning of *N*-terminally truncated *ALG5*
AG5HR1_rv[23]	5'-gcctttggccgaggcggccCGAAAATAAATAGACCAATAAATACAGTG-3'	Cloning of *ALG5* from *N*-terminus to HR1
AG5LR2_rv[23]	5'-gcctttggccgaggcggccgaGTTTCTTATCATTGATCTCTTTATGACG-3'	Cloning of *ALG5* from *N*-terminus to LR2
AG5HR2_rv[23]	5'-gcctttggccgaggcggccgaTGTGTCTTTGATAGACCTGATGCCG-3'	Cloning of *ALG5* from *N*-terminus to HR2
AG5LR3_rv[23]	5'-gcctttggccgaggcggccGCCATCTTAGAGCCATCAACCTC-3'	Cloning of *ALG5* from *N*-terminus to LR3
AG5*ΔN*10_BPfw	5'-tgtaatggccattacggccatgAGAAACACTGTCTTTTTTACGCTCTTAG-3'	Cloning of *ALG5* from HR1 to *C*-terminus
AG5*ΔN*33_BPfw	5'-tgtaatggccattacggccatgTCGCATACACCAAGGCCGCCATATC-3'	Cloning of *ALG5* from LR2 to *C*-terminus

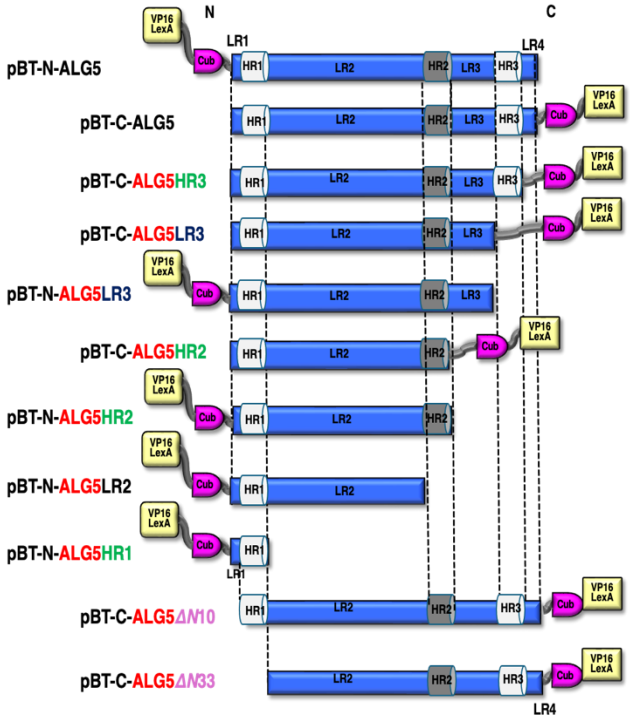

Fig. 1 Bait constructs used in previous and present studies. In structure of expressed Alg5p, bars and boxes indicate loop regions (LRs) and hydrophobic regions (HRs), respectively. Transcription factor VP16/LexA and Cub (C-terminal half of ubiquitin) are added at either *N*- or *C*- terminus of Alg5p.

2.2 *Assays for the physical interaction of Alg5p*

In our previous study, three prey recombinant plasmids (prey constructs), pPR-N-DPM1, pPR-N-SEC59 and pPR-N-CWH8, were prepared for expression of full-length Dpm1p, Sec59p and Cwh8p, respectively[23].

Each of the six novel bait constructs mentioned above was combined with each of the three prey constructs, then they were used for co-transformation of yeast NMY51 strain[33]. After the co-transformation, the co-transformants grown on the synthetic dextrose (SD) medium lacking leucine and tryptophan (SD-LW) were subject to growth examination on the SD medium lacking leucine, tryptophan and histidine (SD-LWH) and SD medium lacking leucine, tryptophan, histidine and adenine (SD-LWHA) according to the manual supplied by Dualsystems Biotech (www. dualsystems.com).

3. Results and Discussion

3.1 *The physical interaction of truncated Alg5p with Sec59p and Cwh8p*

First, we examined growth of co-transformants with pBT-N-ALG5LR3 bait construct (Fig. 1), which would express *N*-terminally tagged Alg5/LR3p lacking the third hydrophobic region (HR3) and the fourth loop region (LR4). In our previous analysis, it has been demonstrated that *C*-terminally tagged Alg5/LR3p could physically interact with Dpm1p, Sec59p and Cwh8p preys[23]. As shown in Fig. 2A, co-transformants expressing Dpm1p and Cwh8p normally grew on two selective media (two red frames), but those expressing Sec59p displayed reduced growth on two selective media (a green frame). This result indicated that HR3 of Alg5p was at least partially related to the physical interaction with Sec59p.

Next, we examined growth of co-transformants with pBT-C-ALG5HR2 bait construct (Fig. 1), which would express *C*-terminally tagged Alg5/HR2p lacking the third loop region (LR3), HR3 and LR4. As shown by a red frame in Fig. 2B, co-transformants expressing Dpm1p were able to grow on two selective media (a red frame), but those expressing Sec59p or Cwh8p were not (a blue frame). Subsequently we examined growth of co-transformants with pBT-N-ALG5HR2 bait construct (Fig. 1), which would express *N*-terminally tagged Alg5/HR2p. As a result, co-transformants expressing Dpm1p or Cwhp1p were able to grow on two selective media (two red frames in Fig. 2C), while those expressing Sec59p were not (a blue frame in Fig. 2C). These observations clearly indicated that LR3 of Alg5p was critical for the interaction with Sec59p and partially contributed to the interaction with Cwh8p.

Co-transformants expressing Cwh8p with *N*-terminally tagged Alg5HR2p survived on the selective media (a lower red frame in Fig. 2C), but those with *N*-terminally tagged Alg5LR2p lacking HR2 seldom survived (a blue frame in Fig.

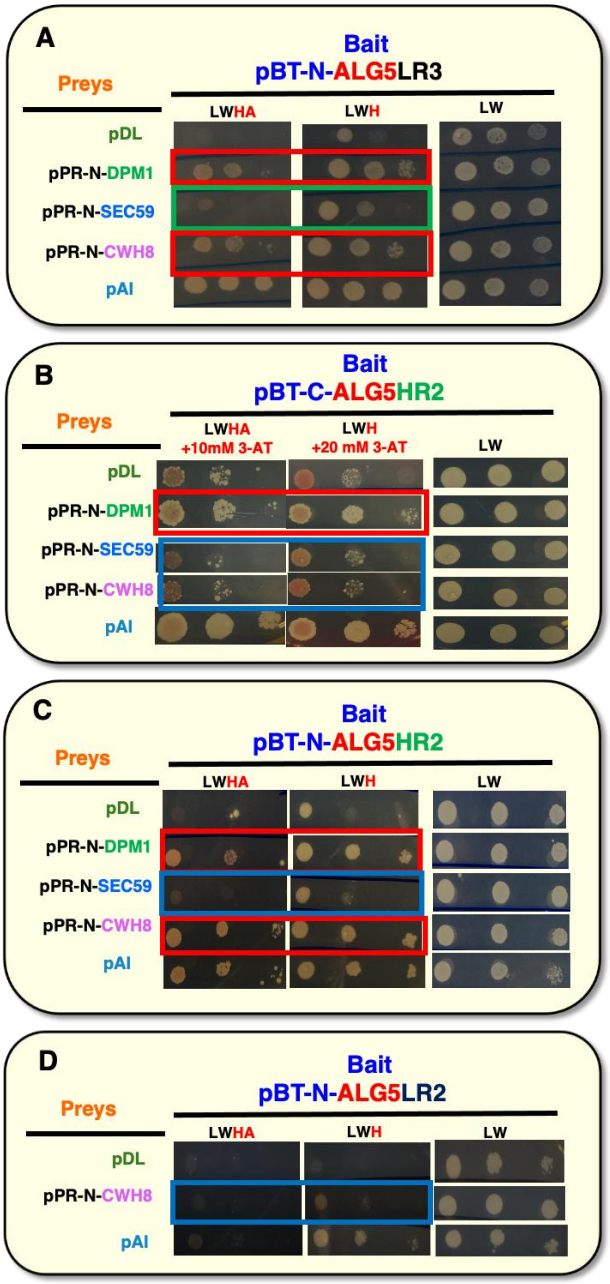

Fig. 2 Growth examination of co-transformants using pBT-N-ALG5LR3 (A), pBT-C-ALG5HR2 (B), pBT-N-ALG5HR2 (C) and pBT-N-ALG5LR2 (D) bait constructs. After the selection of colonies derived from the co-transformants on the SD-LW medium, their suspensions were diluted with sterilized water and adjusted to the OD_{600} values of 1.0, 0.1 and 0.01 (from left to right). These diluents were orderly spotted on the SD-LWH and SD-LWHA media for reporter detection, and SD-LW media for growth control, and then incubated at 30 ºC for 2~4 days.

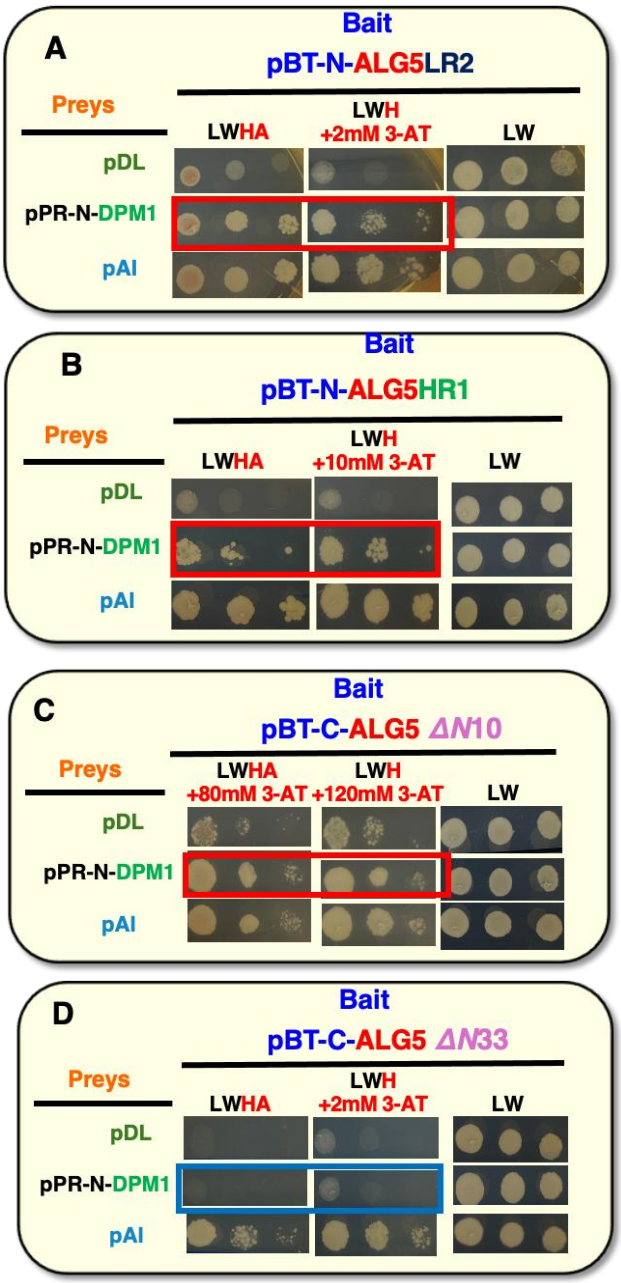

Fig. 3 Growth examination of co-transformants using pBT-N-ALG5LR2 (A), pBT-N-ALG5HR1 (B), pBT-C-ALG5ΔN10 (C) and pBT-C-ALG5ΔN33 (D). The experiments were carried out according to the same procedure as described in the legend of Fig. 2.

Alg5LR2p lacking HR2 seldom survived (a blue frame in Fig.2D). This result means that HR2 of Alg5p would be also required for the interaction with Cwh8p, in addition to LR3. In contrast, LR3 should make no contribution to the interaction with Dpm1p (Fig. 2A and 2B).

3.2 *The physical interaction of truncated Dpm1p*

In order to further refine a region interacting with Dpm1p, we examined growth of co-transformants with novel bait constructs (pBT-N-ALG5LR2 and pBT-N-ALG5HR1) which would express the more truncated Alg5p. For analyzing the membrane topology of Alg5p, we have previously prepared pBT-C-ALG5LR2 and pBT-C-ALG5HR1 bait constructs which would express *C*-terminally tagged Alg5/LR2p ranging from *N*-terminus to the second loop region (LR2) and *C*-terminally tagged Alg5/HR1p ranging from *N*-terminus to the first hydrophobic region (HR1), respectively[23]. However, as it was demonstrated that LexA/VP16-Cub tag in these truncated Alg5p proteins was localized within the rER lumen[23], these bait constructs were proved to be unavailable

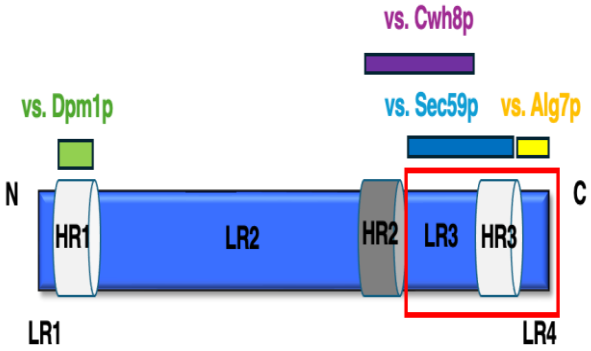

Fig. 4 Summary of interacting regions of Alg5p. A red frame indicates a region that are critical of self-interaction of Alg5p. The interacting regions with Alg5p itself and Alg7p are based on the results of Ref. 23.

for analysis of the physical interaction. Therefore, we newly prepared and used pBT-N-ALG5LR2 and pBT-N-ALG5HR1 bait constructs (Fig. 1) which would express *N*-terminally tagged Alg5/LR2p and *N*-terminally tagged Alg5/HR1p, where LexA/VP16-Cub tags are oriented toward the cytosolic side, respectively. These co-transformants expressing Dpm1p were still able to grow on two selective media (red frames in Fig. 3A and 3B), suggesting that Alg5p should physically interact with Dpm1p via an *N*-terminal portion.

Hence, we tried two additional bait constructs (pBT-C-ALG5 $\Delta N10$ and pBT-C-ALG5 $\Delta N33$) which would express *N*-terminally truncated Alg5p lacking the first 10 and 33 amino acids, respectively (Fig. 1). Because the first loop region (LR1) consists of the first 10 amino acids, and HR1 comprises the following 23 amino acids. As a result of growth examination, co-transformants with pBT-C-ALG5 $\Delta N10$ could still grow on two selective media (a red frame in Fig. 3C), but those with pBT-C-ALG5 $\Delta N33$ could not (a blue frame in Fig. 3D). These findings obviously mean that LR1 of Alg5p is not required for the interaction and that HR1 is necessary and sufficient.

4. Conclusion

In previous study, we detected the physical interactions of Alg5p with Alg5p itself, Dpm1p, Sec59p, Cwh8p. Moreover, we refined Alg5p regions interacting with Alg5p and Alg7p, but unsuccessfully refined those with Sec59p, Cwh8p and Dpm1p. Here, we could achieve the refinement of regions interacting with these three enzymes. Our data obtained from previous and present studies are summarized in Fig. 4.

In the late stages of DLO assembly, both DPM and DPG, which are provided by Dpm1p and Alg5p respectively, are essential. For efficient progression of DLO assembly, these two enzymes might physically interact with each other, and share the common substrate Dol-P in a balanced fashion. Our result that Alg5p interacts with Dpm1p via HR1 (Fig. 4) well agrees with this purpose. By our previous topological analysis, it was revealed that HR1 of Alg5p serves as a transmembrane domain[23]. Therefore it is estimated that the interaction between Alg5p and Dpm1p would be rigider than that via non-transmembrane region.

On the other hand, in order to effectively obtain Dol-P from two providing enzymes (Sec59p and Cwh8p), Alg5p might need to simultaneously interact with them via a different region other than HR1. Interestingly, our data strongly suggest that Alg5p interacts with both via overlapping LR3, which is distal to HR1 (Fig. 4). Perhaps the interactions of LR3 on Alg5p with them would occur in a reciprocal manner. In contrast, the interacting region of Alg5p with Alg7p is another LR4[23], which would not interfere with Dpm1p and Sec59p/Cwh8p (Fig. 4).

More interestingly, a self-interacting region of Alg5p extends from LR3 to LR4, which also overlaps with interacting region with Sec59p, Cwh8p and Alg7p (Fig. 4). This fact raises a possibility that complex formation would be competing among Alg5p, Sec59p, Cwh8p and Alg7p, on the rER membrane. It is estimated that Alg5p/Alg5p complex preferentially forms rather than other complexes, because the interacting region with itself is longer than others. To prove out the possibility, stoichiometric analysis of Alg5p-containing complexes would be required.

We are now progressing analysis of physical interactions between Alg5p and the four enzymes by using prey constructs which would express truncated Dpm1, Sec59p, Cwh8p or Alg7p, to refine regions on them, which are critical for interacting with Alg5p bait. Together with those results, our research should be very significant for elucidation of multiple complexes centering Alg5p on the rER membrane.

References

1) M. Aebi, *N*-linked protein glycosylation in the ER, Biochim. Biophys. Acta Vol.1833, pp.2430-2437 (2013).
2) A. D. Elbein, Inhibitors of the biosynthesis and processing of *N*-linked oligosaccharides, CRC Crit.Rev. Biochem. Vol.16, pp.21-49 (1984).
3) A. Herscovics and P. Orlean, Glycoprotein biosynthesis in yeast, FASEB J. Vol.**7,** pp.540-550 (1993).
4) M. A. Kukuruzinska, M. L. E. Bergh and B. J. Jackson, Protein glycosylation in yeast, Ann. Rev. Biochem. Vol.56, pp.915-944 (1987).
5) C. B. Hirschberg and M. D. Snider, Topography of glycosylation in the rough endoplasmic reticulum and Golgi apparatus, Annu. Rev. Biochem. Vol.56, pp.63-87 (1987).
6) T. Takahashi, Dolichyl-phosphate beta-glucosyltransferase (ALG5), Handbook of glycosyltransferases and related genes, 2nd edition, Springer, chapter146, pp.1649-1655 (2014).
7) G. Palamarczyk, R. Drake, B. Haley and W. J. Lennarz, Evidence that the synthesis of glucosylphospho-dolichol in yeast involves a 35-kDa membrane protein, Proc. Natl. Acad. Sci. USA Vol.87, No.7, pp.2666-2670 (1990).
8) S. te Heesen, L. Lehle, A. Weissmann and M. Aebi, Isolation of the *ALG5* locus encoding the UDP-glucose: dolichyl-phosphate glucosyltransferase from *Saccharomyces cerevisiae*. Eur. J. Biochem. Vol.224, pp.71-79 (1994).

9) N. Johnsson and A. Varshavsky, Split ubiquitin as a sensor of protein interactions *in vivo*, Proc. Natl. Acad. Sci. USA Vol.91, No.22, pp.10340-10344 (1994).
10) I. Stagljar, C. Korostensky, N. Johnsson and S. te Heesen, A genetic system based on split-ubiquitin for the analysis of interactions between membrane proteins *in vivo*, Proc. Natl. Acad. Sci. USA Vol.95, pp.5187-5192 (1998).
11) M. Fetchko and I. Stagljar, Application of the split-ubiquitin membrane yeast two-hybrid system to investigate membrane protein interactions, Methods Vol.32, pp.349-362 (2004).
12) S. Thaminy, J. Miller and I. Stagljar, The split-ubiquitin membrane-based yeast two-hybrid system, Methods. Mol. Biol. Vol.261, pp.297–312 (2004).
13) M. Dünnwald, A. Varshavsky and N. Johnsson, Detection of transient *in vivo* interaction between substrate and transporter during protein translocation into the endoplasmic reticulum, Mol. Biol. Cell Vol.10, pp.329-344 (1999).
14) M. J. Massaad and A. Herscovics, Interaction of the endoplasmic reticulum alpha 1,2-mannosidase Mns1p with Rer1p using the split-ubiquitin system. J. Cell Sci. Vol.114, pp.4629-4635 (2001).
15) W. Scheper, S. Thaminy, S. Kais, I. Stagljar and K. Römisch, Coordination of *N*-glycosylation and protein translocation across the endoplasmic reticulum membrane by Sss1 protein, J. Biol. Chem. Vol.278, No.39, pp.37998-38003 (2003).
16) A. Yan and W. J. Lennarz, Studies on yeast oligosaccharyl transferase subunits using the split-ubiquitin system: Topological features and *in vivo* interactions, Proc. Natl. Acad. Sci. USA Vol.102, No.20, pp.7121-7126 (2005).
17) T. Takahashi and X. -D. Gao, Physical interactions among human glycosyltransferases involved in dolichol-linked oligosaccharide biosynthesis, Trends in Glycoscience and Glycotechnology Vol.24, No.136, pp.65-77 (2012).
18) T. Takahashi, N. Yamada and N. Kurimoto, Analyses on the physical interactions of the human dolichyl-phosphate mannose synthase, Proc. Schl. Eng. Tokai Univ., Ser. J. Vol.57, No.1, pp.5-10 (2017).
19) T. Takahashi and T. Takeuchi, Membrane topological characterization of the human Alg14 protein, Proc. Schl. Eng. Tokai Univ., Ser. E Vol.44, pp.1-6 (2019).
20) T. Takahashi, K. Nishimura, N. Maeda and R. Oshiro, Characterization of the membrane topology and physical interaction of human *N*-acetylglucosamine-1-phosphate transferase, Proc. Schl. Eng. Tokai Univ., Ser. E Vol.46, pp.1-6 (2021).
21) T. Takahashi, N. Yamada and R. Oshiro, Characterization of the membrane topology and physical interaction of human dolichol-phosphate-glucose synthase, Proc. Schl. Eng. Tokai Univ., Ser. E Vol.47, pp.1-6 (2022).
22) Samantha, M. Ismail, A. Takeshima and T. Takahashi, Construction of a novel set of control preys for the yeast split-ubiquitin system, Eng. Tokai Univ., Ser. E Vol.48, pp.1-5 (2023).
23) Samantha and T. Takahashi, Analyses of the membrane topology and physical interactions of yeast dolichyl-phosphate glucose synthase Alg5p, Proc. Schl. Eng. Tokai Univ., Ser. E Vol.49, pp.19-25 (2024).
24) P. Orlean, Dolichol phosphate mannose synthase is required *in vivo* for glycosyl phosphatidylinositol membrane anchoring, *O*-mannosylation, and *N*-glycosylation of protein in *Saccharomyces cerevisiae*, Mol. Cell. Biol. Vol.10, pp.5796-5805 (1990).
25) T. Takahashi, Dolichyl-phosphate mannosyltransferase polypeptide (DPM1-3), Handbook of glycosyltransferases and related genes, 2nd edition, Springer, chapter146, pp.1637-1647 (2014).
26) G. Barnes, W. J. Hansen, C. L. Holcomb and J. Rine, Asparagine-linked glycosylation in *Saccharomyces cerevisiae*: genetic analysis of an early step, Mol. Cell. Biol. Vol.4, pp.2381-2388 (1984).
27) L. Heller, P. Orlean and W. L. Adair Jr., *Saccharomyces cerevisiae sec59* cells are deficient in dolichol kinase activity, Proc. Natl. Acad. Sci. USA Vol.89, pp.7013-7016 (1992).
28) M. A. A. van Berkel, M. Rieger, S. te Heesen, A. F. J. Ram, H. van dn Ende, M. Aebi and F. M. Klis, The *Saccharomyces cerevisiae CWH8* gene is required for full levels of dolichol-linked oligosaccharides in the endoplasmic reticulum and efficient *N*-glycosylation, Glycobiology Vol.9, No.3, pp.243-253 (1999).
29) F. Fernandez, J. S. Rush, D. A. Toke, G.-soo Han, J. E. Quinn, G. M. Carman, J.-Y. Choi, D. R. Voelker, M. Aebi and C. J. Waechter, The *CWH8* gene encodes a dolichyl pyrophosphate phosphatase with a luminally oriented active site in the endoplasmic reticulum of *Saccharomyces cerevisiae*, J. Biol. Chem. Vol.276, No.44, pp.41455-41464 (2001).
30) H. A. Erlich, PCR Technology, Stockton Press, pp.61-70 (1989).
31) H. Inoue, H. Nojima and H. Okayama, High efficiency transformation of *Escherichia coli* with plasmids, Gene Vol.96, pp.23–28 (1990).
32) L. Sambrook, E. F. Fritsch and T. Maniatis, Molecular Cloning: A Laboratory Manual. Second edition, Cold Spring Harbor Laboratory Press, NY, (1989).
33) H. Ito, Y. Fukuda, K. Murata and A. Kimura, Transformation of intact yeast cells treated with alkali cations, J. Bacteriol. Vol.153, No.1, pp.163-168 (1983).

Proc. Schl. Eng. Tokai Univ., Ser. E
50 (2025) 13-17
DOI: 10.18995/24343641. 50. 13

Characterization of the Membrane Topology of Human Chitobiosyldiphosphodolichol Beta-1,4-Mannosyltransferase

by

Tetsuo TAKAHASHI[*1], Takana MIYAZAKI[*2] and Kazunobu SASAKI[*2]

(Received on Mar. 24, 2025 and accepted on Jun. 20, 2025)

Abstract

In the assembly of dolichol-linked oligosaccharide (DLO), human chitobiosyldiphosphodolichol beta-1,4-mannosyltransferase (hMT-I, EC 2.4.1.142) catalyzes the transfer of mannose (Man) from GDP-Man to chitobiosyldiphosphodolichol ($GlcNAc_2$-PP-dolichol) to generate $Man_1GlcNAc_2$-PP-dolichol. We have already cloned the *HMT-1* gene, which encodes this enzyme, and conducted mutational analysis. Here, by applying the gene to the yeast split-ubiquitin system (YSUS), we investigated the membrane topology of hMT-I. Our results strongly suggested that this enzyme has a single transmembrane domain with the *N*-terminus and *C*-terminus oriented toward the lumen and cytosol, respectively.

***Keywords*:** Beta-1,4 mannosyltransferase, Membrane topology, Split-ubiquitin system

1. Introduction

The biosynthesis of dolichol-linked oligosaccharides (DLOs) on the rough endoplasmic reticulum (rER) membrane is a process that critical for the protein *N*-glycosylation in eukaryotes, and therefore evolutionally well conserved from yeast to mammals including human[1-5]. In the early stage of assembly of DLO, the intermediate DLO, $Man_5GlcNAc_2$-PP-dolichol, which is half-sized DLO, are formed by five glycosyltransferase (Fig. 1). Of them, chitobiosyldiphospho-dolichol beta-1,4-mannosyltransferase (MT-I, EC 2.4.1.142) plays a role in the first mannosylation of DLO. We previously cloned the *HMT-1* gene which encodes human MT-I (hMT-I), as a guide to complementing activity of yeast *alg1* mutation[6]. Moreover, concerning the *HMT-1* gene and hMT-I, we have conducted mutational analysis of *HMT-1* to explore the functional motifs of hMT-I[7], investigated upstream regions and elements of *HMT-1* gene, which are critical for its transcriptional regulation[8], and investigated the physical interactions of hMT-I among the five glycosyltransferases involved in the early stage of DLO assembly[9] using the yeast split-ubiquitin system (YSUS)[10-14]. The YSUS is a technique which can detect not only the physical interaction between two membrane proteins but the membrane topology of a bait membrane protein[15-24]. In this study, we tried to clarify the membrane topology of hMT-I by using deletional mutants of *HMT-1* for the YSUS.

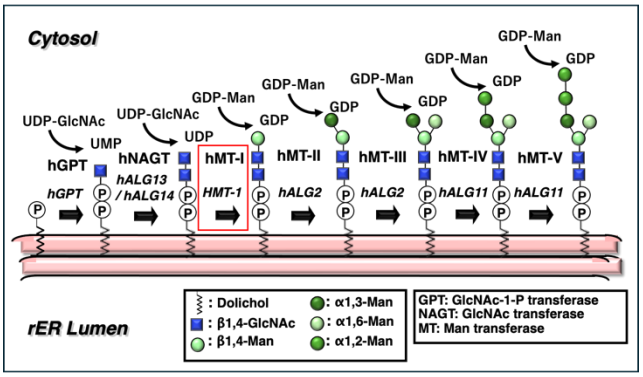

Fig. 1 Early stage of human dolichol-linked oligo-saccharide (DLO) biosynthesis. The upper names and lower italic names above arrows mean human enzymes and genes, respectively.

2. Experimental Methods

2.1 Computational *prediction of the membrane topology of hMT-1*

In order to predict the membrane topology of the hMT-I protein, three WWW algorithms servers, Phobius (https://phobius.sbc.su.se/cgi-bin/predict.pl)[25], TMAP (https://embossgui.sourceforge.net/demo/manual/tmap.html)[26),27] and PRED-TMR (http://athina.biol.uoa.gr/PRED-TMR/)[28] were used. On its WEB site, the amino acid sequence of the hMT-I protein consisting of 464 residues was registered and surveyed for its potential transmembrane domain (TMD) and membrane topology.

*1 Associate Professor, Department of Bioengineering
*2 Undergraduate Student, Department of Applied Biochemistry

Table I The PCR primers used in this study. Additional sequences containing a *Sfi* I- cleavage site are shown in lowercase letters.

Primer name	Nucleotide sequence	Purpose
A1BP-F	5'-tgtaatggccattacggccATGGCGGCCTCATGCTTGGTC-3'	Construction of pBT-STE-A1dx series
A1d1BP-R	5'-gcctttggccgaggcggccCGCGTGGTACTGCATACGGGGG-3'	Construction of pBT-STE-A1d1
A1 d2BP-R	5'-gcctttggccgaggcggccGAGTTGCAGAACCCCAGGAGG-3'	Construction of pBT-STE-A1d2
A1 d3BP-R	5'-gcctttggccgaggcggccCTCCCTCCACATCAACTTCCAC-3'	Construction of pBT-STE-A1d3
A1 d4BP-R	5'-gcctttggccgaggcggccGGCAGACCTGGGGGGTTCTGG-3'	Construction of pBT-STE-A1d4
A1 d5BP-R	5'-gcctttggccgaggcggccACGAGCTTGCTTCCACAAAGG-3'	Construction of pBT-STE-A1d5
A1 d6BP-R	5'-gcctttggccgaggcggccCATGATGGAGTAGCCATAGTTG-3'	Construction of pBT-STE-A1d6

2.2 *Construction of recombinant plasmids for expression of truncated hMT-I baits*

In our previous study, we prepared two bait recombinant plasmids (bait constructs), pBT-N-A1 and pBT-STE-A1, for expression of full-length hMT-I which were tagged at *N*- and *C*- terminus, respectively[9], via a PCR using A1BP-F and A1BP-R primers listed in Table 1. In this study, we prepared six bait constructs (pBT-STE-A1d1, pBT-STE-A1d2, pBT-STE-A1d3, pBT-STE-A1d4 pBT-STE-A1d5 and pBT-STE-A1d6) which would express *C*-terminally truncated hMT-I (Fig. 5). For cloning, PCRs were performed using forward primer A1BP-F and each of reverse primers (A1d1BP-R to A1d6BP-R) by standard method[29] and then amplified DNA fragments were cloned into the pBT-STE vector. PCR primers are listed in Table 1, and DNA cloning was conducted according to the same procedure as previously described[30),31].

2.3 *Assays for the membrane topology of hMT-I*

Six pBT-STE-A1dx series and two pBT-N-dxA1 series, which were prepared as described in section 2.1, were used for co-transformation of the *Saccharomyces cerevisiae* NMY51 strain, together with the positive or negative control prey construct, pAI-Alg5 or pDL-Alg5. The transformation of the yeast cells was carried out by the standard method[32]. The co-transformants obtained on the synthetic dextrose (SD) medium lacking leucine and tryptophan (SD-LW) were then subject to the growth examination on the SD medium lacking leucine, tryptophan and histidine (SD-LWH) and SD medium lacking leucine, tryptophan, histidine and adenine (SD-LWHA) according to the manual supplied by Dualsystems Biotech (www.dualsystems.com).

3. Results and Discussion

3.1 *Prediction of the membrane topology of hMT-I*

hMT-I protein is composed of 464 amino acid residues. We started from predicting the membrane topology of hMT-I protein using three algorithms servers which are freely available on WEB sites. As shown in Fig. 2, Phobius predicted three hydrophobic regions (violet peaks), which are potential TMDs, in *N*-terminal half of hMT-I protein. It also predicted that *N*- and *C*- termini of hMT-I would be oriented towards lumen and cytoplasm, respectively. TMAP predicted

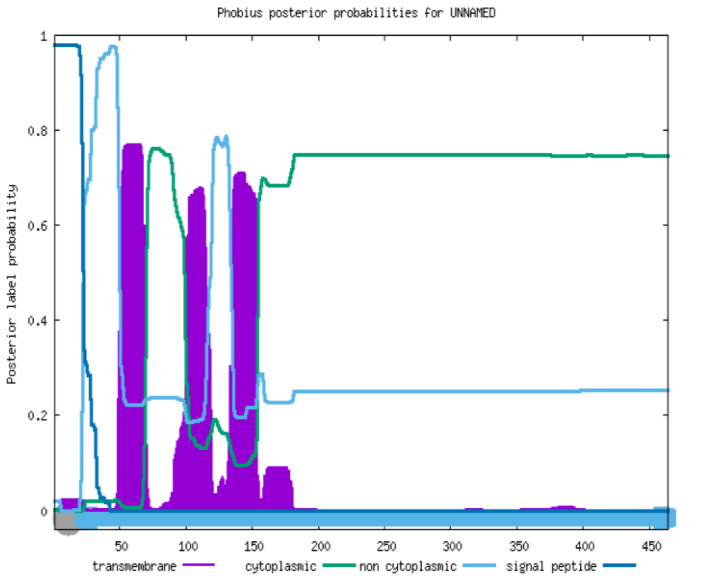

Fig. 2 Results from Phobius prediction of the membrane topology and TMDs in hMT-I.

three TMDs, too. However, the first TMD predicted by TMAP was different from that by Phobius (Fig. 3). Moreover, PRED-TMR also predicted three TMDs, but represented TMD-predicted pattern different from both Phobius and TMAP (Fig. 4). Results of these predictions are summarized in Fi. 5. Consequently, we detected four TMD candidates in hMT-I and designated them as hydrophobic regions (HRs) 1 to 4 (Fig. 5). Based on these predictions, we chose six positions, to which Cub-LexA/VP16 tag were added, in hMT-I, and newly prepared six bait constructs (pBT-STE-A1dx ; x is any number from 1 to 6) that would express *C*-terminally truncated hMT-I proteins (Fig. 5). The *C*-terminally truncated hMT-Is expressed by pBT-STE-A1d1, pBT-STE-A1d2 and pBT-STE-A1d3 would just contain HR1, HR1/HR2 and HR1/HR2/HR3, respectively. hMT-I expressed by pBT-STE-A1d4 would contain the second conserved motif II, an addition to HR1/HR2/HR3. hMT-I expressed by pBT-STE-A1d5 would contain HR1/HR2/HR3/HR4, and that by pBT-STE-A1d6 would contain the third conserved motif III in addition to HR1/HR2/HR3/HR4 (Fig. 5). To experimentally determine TMD in hMT-I, these bait constructs

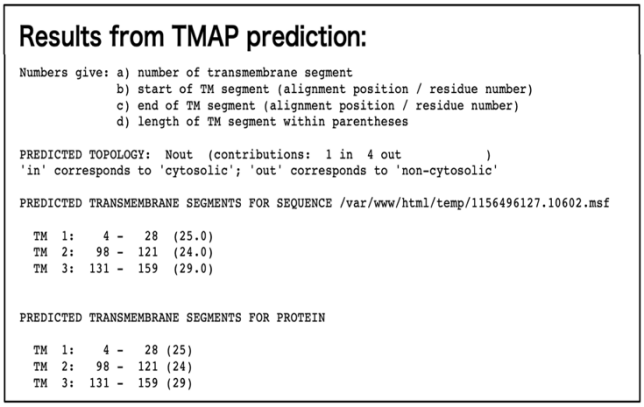

Results from TMAP prediction:

```
Numbers give: a) number of transmembrane segment
              b) start of TM segment (alignment position / residue number)
              c) end of TM segment (alignment position / residue number)
              d) length of TM segment within parentheses

PREDICTED TOPOLOGY:  Nout  (contributions:  1 in  4 out           )
'in' corresponds to 'cytosolic'; 'out' corresponds to 'non-cytosolic'

PREDICTED TRANSMEMBRANE SEGMENTS FOR SEQUENCE /var/www/html/temp/1156496127.10602.msf

  TM  1:    4 -   28  (25.0)
  TM  2:   98 -  121  (24.0)
  TM  3:  131 -  159  (29.0)


PREDICTED TRANSMEMBRANE SEGMENTS FOR PROTEIN

  TM  1:    4 -   28 (25)
  TM  2:   98 -  121 (24)
  TM  3:  131 -  159 (29)
```

Fig. 3 Results from TMAP prediction of TMDs in hMT-I.

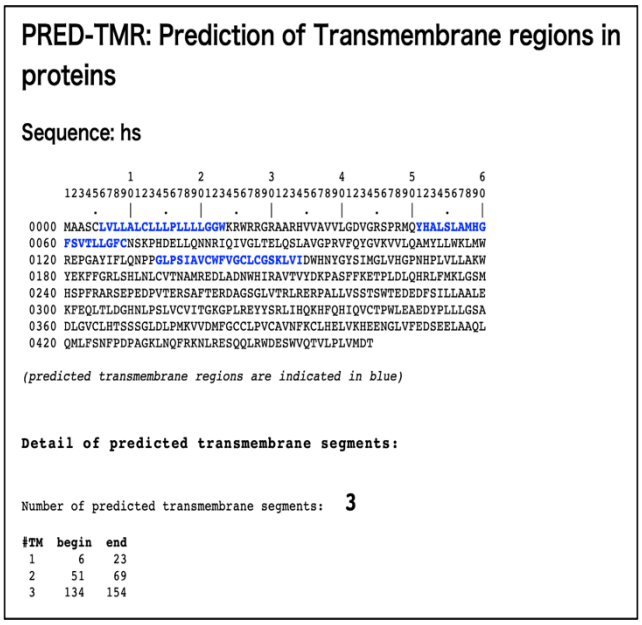

PRED-TMR: Prediction of Transmembrane regions in proteins

Sequence: hs

```
                1         2         3         4         5         6
      1234567890123456789012345678901234567890123456789012345678901234567890
          .    |    .    |    .    |    .    |    .    |    .    |    .    |
 0000 MAASCLVLLALCLLLPLLLLGGWKRWRRGRAARHVVAVVLGDVGRSPRMQYHALSLAMHG
 0060 FSVTLLGFCNSKPHDELLQNNRIQIVGLTELQSLAVGPRVFQYGVKVVLQAMYLLWKLMW
 0120 REPGAYIFLQNPPGLPSIAVCWFVGCLCGSKLVIDWHNYGYSIMGLVHGPNHPLVLLAKW
 0180 YEKFFGRLSHLNLCVTNAMREDLADNWHIRAVTVYDKPASFFKETPLDLQHRLFMKLGSM
 0240 HSPFRARSEPEDPVTERSAFTERDAGSGLVTRLRERPALLVSSTSWTEDEDFSILLAALE
 0300 KFEQLTLDGHNLPSLVCVITGKGPLREYYSRLIHQKHFQHIQVCTPWLEAEDYPLLLGSA
 0360 DLGVCLHTSSSGLDLPMKVVDMFGCCLPVCAVNFKCLHELVKHEENGLVFEDSEELAAQL
 0420 QMLFSNFPDPAGKLNQFRKNLRESQQLRWDESWVQTVLPLVMDT
```

(predicted transmembrane regions are indicated in blue)

Detail of predicted transmembrane segments:

Number of predicted transmembrane segments: **3**

#TM	begin	end
1	6	23
2	51	69
3	134	154

Fig. 4 Results from PRED-TMR prediction of TMDs in hMT-I.

were then subject to analysis of membrane topology by the YSUS.

3.2 *Analysis of the membrane topology of hMT-I*

We examined the growth of co-transformants with pBT-STE-A1dx series which would express *C*-terminally truncated hMT-I on the two selective media. It is necessary to orient Cub-LexA/VP16 tag fused with hMT-I expressed in yeast cells towards the cytosol for growth on two selective media (SD-LWH and SD-LWHA)[10-14]. We have previously conducted growth examination of the co-transformants using pBT-N-A1 and pBT-STE-A1, which would express full-length hMT-I *N*- and *C*-terminally tagged with Cub/LexA, respectively. When combined with positive control prey construct pAI-Alg5, co-transformants of pBT-N-A1 did not grow on the selective media, while those of pBT-STE-A1 grew (Ref. 9 and Fig. 6). These results obviously indicated that *N*-terminus of hMT-I was oriented towards the lumen and *C*-terminus was oriented towards the cytoplasm. Therefore, a

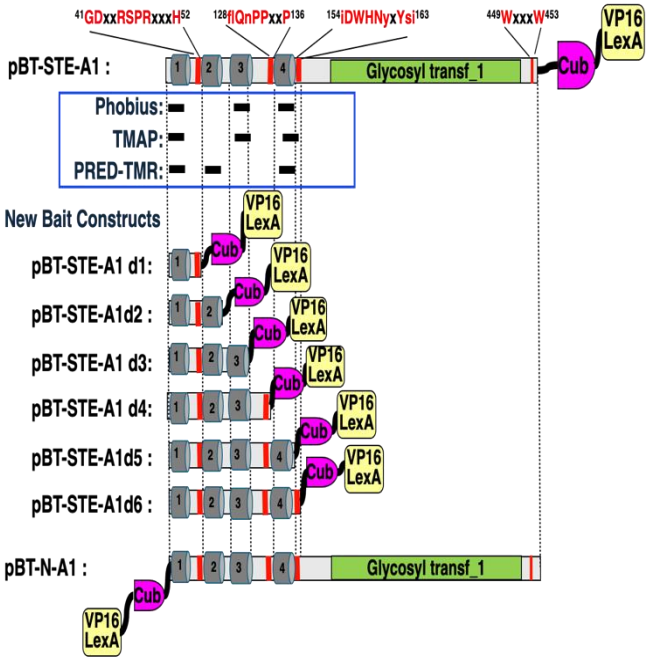

Fig. 5 Bait constructs and expressed truncated hMT-I. Based on the predictions of TMDs by Phobius, TMAP and PRED-TMR (a blue frame), grey boxes with number indicate hydrophobic regions (HRs) in hMT-I expressed by each bait construct. Transcription factor VP16/LexA and Cub (C-terminal half of ubiquitin) are added at either *N*- or *C*-terminus of hMT-I. Four conserved motifs (I to IV) are indicated by red bars. A green region indicates a catalytic domain.

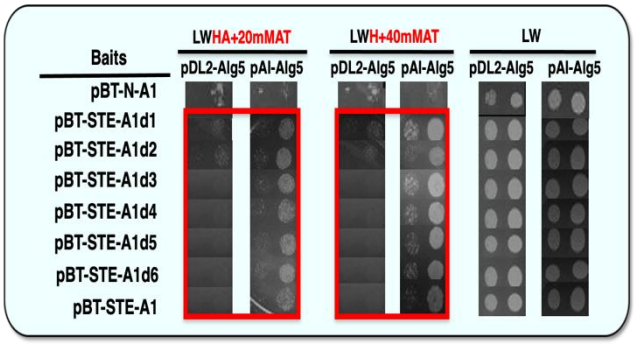

Fig. 6 Growth examination of co-transformants using pBT-STE-A1dx series. After the selection of colonies derived from the co-transformants on the SD-LW medium, their suspensions were diluted with sterilized water and adjusted to the OD_{600} values of 1.0 and 0.1 (from right to left). These diluents were orderly spotted on the SD-LWH and SD-LWHA media for reporter detection, and SD-LW media for growth control, and then incubated at 30 ºC for 2~4 days.

positional prediction of termini of hMT-I by Phobius well matched our results. Co-transformants with pBT-STE-A1d1 and pAI-Alg5 grew on the media as well as those with pBT-STE-A1 and pAI-Alg5 (two red frames in Fig. 6), indicating that the position after HR1 and before HR2 was located in the cytosol. Co-transformants with pBT-STE-A1d2 and pAI-Alg5 similarly grew on the media (two red frames in Fig. 6), indicating that the position after HR2 and before HR3

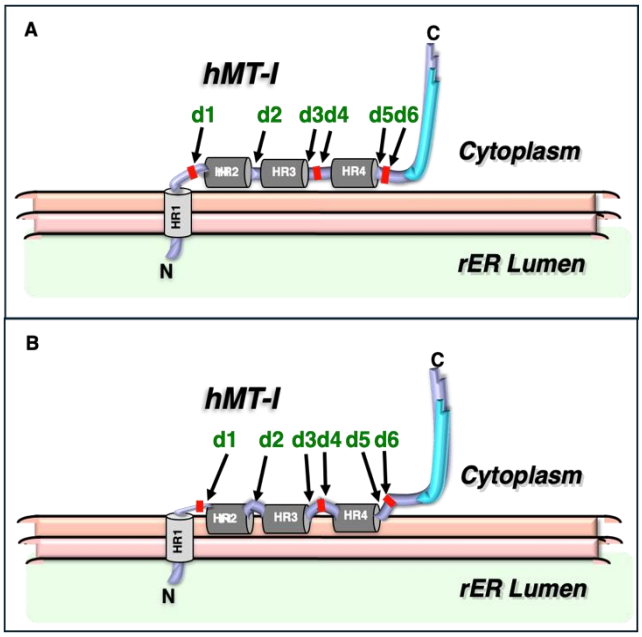

Fig. 7 Models of the membrane topology of hMT-I. Arrows indicate positions at which Cub-LexA/VP16 tag was added in truncated hMT-I which expressed by six bait constructs. Three red bars indicate positions of the conserved motifs I to III. A blue region indicates a catalytic domain.

was in the cytosol. Hence, HR2 would not function as a TMD. As well, HR3 and HR4 were estimated to be non-TMDs, because co-transformants from pBT-STE-A1d3 to pBT-STE-A1d6 also grew on the media when combined with pAI-Alg5 (two red frames in Fig. 6). These observations indicated that the positions after HR3, before HR4, and after HR4 were located in the cytosol. Therefore, our results suggested that hMT-I had only one TMD and that it should be HR1.

4. Conclusion

In the previous study, we estimated that hMT-I has three TMDs consisting of HR1, HR3 and HR4[7]. However, here, we analyzed the membrane topology of hMT-I and concluded that it possessed one TMD, corresponding to HR1, with *N*- and *C*- termini localized in the rER lumen and cytoplasm, respectively. Based on our data obtained from present study, we propose two models represented in Fig. 7. Both models support that hMT-I is substantially an ER integral membrane protein with type I topology[33]. It is also possible that either of HR2, HR3 and HR4 would contact with the membrane or dip in the membrane. In any case, three conserved motifs I to III were demonstrated to be located in the cytosol.

In previous study, we identified hALG2, hALG11, and hALG13 as enzymes that physically interacted with hMT-I[9]. In model A of Fig. 7, HR2, HR3 and HR4 would be located near the rER membrane or weakly associated with surface of the membrane. If these HRs transiently participate in the physical interactions of itself or other enzymes, their positioning might have a great advantage in flexibility. On the other hand, they might be dipped in the outer leaf of bilayer of the rER membrane in model B. In this case, these HRs might contribute to tightly interacting with the enzymes. We are now investigating whether these HRs and motifs are important for the interactions with hALG2, hALG11 and hALG13.

A number of reports have demonstrated that the defect of *HMT-1* gene causes congenital disorder of glycosylation type Ik (CDG-Ik or CDG-ALG1)[34-40]. In some cases, mutated sites were identified out of catalytic domains. Hence, our data concerning the membrane topology and physical interaction would be expected for contribution to elucidating the mechanism of deficiency of hMT-I function.

References

1) M. Aebi, *N*-linked protein glycosylation in the ER, Biochim. Biophys. Acta Vol.1833, pp.2430-2437 (2013).
2) A. D. Elbein, Inhibitors of the biosynthesis and processing of *N*-linked oligosaccharides, CRC Crit.Rev. Biochem. Vol.16, pp.21-49 (1984).
3) A. Herscovics and P. Orlean, Glycoprotein biosynthesis in yeast, FASEB J. Vol.**7,** pp.540-550 (1993).
4) M. A. Kukuruzinska, M. L. E. Bergh and B. J. Jackson, Protein glycosylation in yeast, Ann. Rev. Biochem. Vol.56, pp.915-944 (1987).
5) C. B. Hirschberg and M. D. Snider, Topography of glycosylation in the rough endoplasmic reticulum and Golgi apparatus, Annu. Rev. Biochem. Vol.56, pp.63-87 (1987).
6) T. Takahashi and R. Honda, Cloning of the human cDNA which can complement the defect of the yeast mannosyltransferase I-deficient mutant, alg1, Glyco-biology Vol.10, pp.321-327 (2000).
7) T. Miki, M. Uzawa and T. Takahashi, Mutational analyses of the human mannosyltransferase I, Proc. Schl. Eng. Tokai Univ., Ser/ E Vol.42, pp.1-7 (2017).
8) T. Takahashi, T. Nedachi, T. Etoh, H. Tachikawa and X. -D. Gao, Identification and characterization of transcriptional control region of the human beta 1,4-mannosyltransfrase gene, Cytotechnology Vol.69, No.3, pp.417-434 (2017).
9) T. Takahashi and X. -D. Gao, Physical interactions among human glycosyltransferases involved in dolichol-linked oligosaccharide biosynthesis, Trends in Glycoscience and Glycotechnology Vol.24, No.136, pp.65-77 (2012).
10) N. Johnsson and A. Varshavsky, Split ubiquitin as a sensor of protein interactions *in vivo*, Proc. Natl. Acad. Sci. USA Vol.91, No.22, pp.10340-10344 (1994).
11) I. Stagljar, C. Korostensky, N. Johnsson and S. te Heesen, A genetic system based on split-ubiquitin for the analysis of interactions between membrane proteins *in vivo*, Proc. Natl. Acad. Sci. USA Vol.95, pp.5187-5192 (1998).
12) M. Fetchko and I. Stagljar, Application of the split-ubiquitin membrane yeast two-hybrid system to investigate membrane protein interactions, Methods Vol.32, pp.349-362 (2004).
13) S. Thaminy, J. Miller and I. Stagljar, The split-ubiquitin membrane-based yeast two-hybrid system, Methods. Mol. Biol. Vol.261, pp.297–312 (2004).

14) M. Dünnwald, A. Varshavsky and N. Johnsson, Detection of transient *in vivo* interaction between substrate and transporter during protein translocation into the endoplasmic reticulum, Mol. Biol. Cell Vol.10, pp.329-344 (1999).
15) M. J. Massaad and A. Herscovics, Interaction of the endoplasmic reticulum alpha 1,2-mannosidase Mns1p with Rer1p using the split-ubiquitin system. J. Cell Sci. Vol.114, pp.4629-4635 (2001).
16) W. Scheper, S. Thaminy, S. Kais, I. Stagljar and K. Römisch, Coordination of *N*-glycosylation and protein translocation across the endoplasmic reticulum membrane by Sss1 protein, J. Biol. Chem. Vol.278, No.39, pp.37998-38003 (2003).
17) A. Yan and W. J. Lennarz, Studies on yeast oligosaccharyl transferase subunits using the split-ubiquitin system: Topological features and *in vivo* interactions, Proc. Natl. Acad. Sci. USA Vol.102, No.20, pp.7121-7126 (2005).
18) T. Takahashi, N. Yamada and N. Kurimoto, Analyses on the physical interactions of the human dolichyl-phosphate mannose synthase, Proc. Schl. Eng. Tokai Univ., Ser. J. Vol.57, No.1, pp.5-10 (2017).
19) T. Takahashi and T. Takeuchi, Membrane topological characterization of the human Alg14 protein, Proc. Schl. Eng. Tokai Univ., Ser. E Vol.44, pp.1-6 (2019).
20) T. Takahashi, K. Nishimura, N. Maeda and R. Oshiro, Characterization of the membrane topology and physical interaction of human *N*-acetylglucosamine-1-phosphate transferase, Proc. Schl. Eng. Tokai Univ., Ser. E Vol.46, pp.1-6 (2021).
21) T. Takahashi, N. Yamada and R. Oshiro, Characterization of the membrane topology and physical interaction of human dolichol-phosphate-glucose synthase, Proc. Schl. Eng. Tokai Univ., Ser. E Vol.47, pp.1-6 (2022).
22) Samantha, M. Ismail, A. Takeshima and T. Takahashi, Construction of a novel set of control preys for the yeast split-ubiquitin system, Eng. Tokai Univ., Ser. E Vol.48, pp.1-5 (2023).
23) T. Takahashi, E. Horigome, T. Yamanoto and K. Terajima, Analyses of the membrane topology and physical interaction of human dolichol kinase, Proc. Schl. Eng. Tokai Univ., Ser. E Vol.49, pp.13-18 (2024).
24) Samantha and T. Takahashi, Analyses of the membrane topology and physical interactions of yeast dolichyl-phosphate glucose synthase Alg5p, Proc. Schl. Eng. Tokai Univ., Ser. E Vol.49, pp.19-25 (2024).
25) L. Käll, A. Krogh and E. L. L. Sonnhammer, A combined transmembrane topology and signal peptide prediction method. J. Mol. Biol. Vol.338, pp.1027–1036 (2004).
26) B. Persson and P. Argos, Prediction of transmembrane segments in proteins utilising multiple sequence alignments, J. Mol. Biol. Vol.237, pp.182-192 (1994).
27) B. Persson and P. Argos, Topology prediction of membrane proteins, Prot. Sci. Vol.5, pp.363-371 (1996).
28) Hamodrakas and S. J. Hamodrakas, A novel method for predicting transmembrane segments in proteins based on a statistical analysis of the SwissProt database: the PRED-TMR algorithm, Protein Eng. Vol.12, No.5, pp.381-385 (1999).
29) H. A. Erlich, PCR Technology, Stockton Press, pp.61-70 (1989).
30) H. Inoue, H. Nojima and H. Okayama, High efficiency transformation of *Escherichia coli* with plasmids, Gene Vol.96, pp.23–28 (1990).
31) L. Sambrook, E. F. Fritsch and T. Maniatis, Molecular Cloning: A Laboratory Manual. Second edition, Cold Spring Harbor Laboratory Press, NY, (1989).
32) H. Ito, Y. Fukuda, K. Murata and A. Kimura, Transformation of intact yeast cells treated with alkali cations, J. Bacteriol. Vol.153, No.1, pp.163-168 (1983).
33) V. Goder and M. Spiess, Topogenesis of membrane proteins: determinants and dynamics, FEBS Lett. Vol.504, No.3, pp.87-92 (2001).
34) C. E. Grubenmann, C. G. Frank, A. J. Hülsmeier, E. Schollen, G. Matthijs, E. Mayatepek, E. G. Berger, M. Aebi and T. Hennet, Deficiency of the first mannosylation step in the *N*-glycosylation pathway causes congenital disorder of glycosylation type Ik, Hum. Mol. Genet. Vol.13, pp.535–542 (2004).
35) C. Kranz, J. Denecke, L. Lehle, K. Sohlbach, S. Jeske, F. Meinhardt, R. Rossi, S. Gudowius and T. Marquardt, Congenital disorder of glycosylation type Ik (CDG-Ik): a defect of mannosyltransferase I, Am. J. Hum. Genet. Vol.74, pp.545–551 (2004).
36) M. Schwarz, C. Thiel, J. Lübbehusen, B. Dorland, T. de Koning, K. von Figura, L. Lehle and C. Körner, Deficiency of GDP-Man: GlcNAc2-PP-dolichol mannosyltransferase causes congenital disorder of glycosylation type Ik, Am. J. Hum. Genet. Vol.74, pp.472–481 (2004).
37) T. Dupré, S. Vuillaumier-Barrot, I. Chantret, H. S. Yayé, C. Le Bizec, A. Afenjar, C. Altuzarra, C. Barnérias, L. Burglen, P. de Lonlay, F. Feillet, S. Napuri, N. Seta and S. E. H. Moore, Guanosine diphosphate-mannose: GlcNAc2-PP-dolichol mannosyltransferase deficiency (congenital disorders of glycosylation type Ik): five new patients and seven novel mutations, J. Med. Genet. Vol.47, pp.729–735 (2010).
38) T. M. Snow, C. W. Woods and A. G. Woods, Congenital disorder of glycosylation: a case presentation, Adv. Neonatal Care Vol.12, pp.96–100 (2012).
39) A. K. Rohlfing, S. Rust, J. Reunert, M. Tirre, I. Du Chesne, S. Wemhoff, F. Meinhardt, H. Hartmann, A. M. Das and T. Marquardt, ALG1-CDG: a new case with early fatal outcome, Gene Vol.534, pp.345–351(2014).
40) E. Morava, J. Vodopiutz, D. J. Lefeber, A. R. Janecke, W. M. Schmidt, S. Lechner, C. B. Item, J. Sykut-Cegielska, M. Adamowicz, J. Wierzba, Z. H. Zhang, I. Mihalek, S. Stockler, O. A. Bodamer, L. Lehle and R. A. Wevers, Defining the phenotype in congenital disorder of glycosylation due to *ALG1* mutations, Pediatrics Vol.130, e1034–e1039 (2012).

Proc. Schl. Eng. Tokai Univ., Ser. E
50 (2025) 19-23
DOI: 10.18995/24343641. 50. 19

Characterization of the Membrane Topology and Self-Interaction of Yeast Dolichol Kinase Sec59p

by

Tetsuo TAKAHASHI [*1], Koki KURIHARA[*2] and Yu SHIRAIWA[*3]

(Received on Mar. 31, 2025 and accepted on Jun. 20, 2025)

Abstract

For the assembly of dolichol-linked oligosaccharide (DLO) in the eukaryotic cell, dolichyl phosphate (Dol-P) is required and it is *de novo* provided by dolichol kinase (DK). In this study, we cloned the *SEC59* gene, which encodes yeast DK, Sec59p, and analyzed the membrane topology and physical interaction of Sec59p, using the yeast split-ubiquitin system (YSUS). Our research revealed that Sec59p has at least twelve transmembrane domains (TMDs) with both termini oriented toward the cytoplasmic side of the rough ER (rER) membrane. In addition, it was revealed that Sec59p physically interacts with itself, suggesting that it might function in the form of a homodimer.

***Keywords*:** Dolichol kinase, Membrane topology, Physical interaction, Split-ubiquitin system

1. Introduction

In eukaryotes the dolichol cycle serves for biosynthesis of dolichol-linked oligosaccharides (DLOs), which is essential for the protein *N*-glycosylation on the rough endoplasmic reticulum (rER) membrane[1]. In the cycle, the dolichol kinase (DK or DOLK) produces dolichyl-phosphate (Dol-P), which directly serves as a scaffold for the assembly of an oligosaccharide portion of DLO on the rER membrane[2-4]. Namely Dol-P is utilized as an acceptor substrate by GlcNAc-1-P transferase (GPT) that is the first enzyme for assembly of DLO. Dol-P is also utilized as an acceptor substrate by dolichyl-phosphate mannose synthase (DPMS) and dolichyl-phosphate glucose synthase (DPGS), which provides donor substrates with luminal mannosyl-transferases and glucosyltransferases in the cycle, respectively[1].

The gene encoding DK was firstly isolated from *Saccharomyces cerevisiae* as *SEC59* gene[2),3)]. Later, a human orthologous gene of *SEC59* was identified as *hDK1*[4]. Yeast Sec59p encoded by *SEC59* gene consists of 519 amino acids[4] and shows significant homology to human DK (hDK). The overexpression of the *hDK1* cDNA in yeast *sec59* mutant cells could complement the deficiency of yeast DK, demonstrating that enzymatic function is also conserved between yeast and human[4].

We have been investigating the physical interaction of human enzymes involved in dolichol cycle using the yeast split-ubiquitin system (YSUS)[5-8], which has so far identified the physical interaction of various membrane proteins with other membrane proteins[9-18]. Recently, we have reported characterization of the membrane topology and physical interaction of hDK[19]. Here, we investigated those of Sec59p.

*1 Associate Professor, Department of Bioengineering
*2 Undergraduate Student, Department of Bioengineering
*3 Graduate Student, Course of Applied Science and Chemistry

2. Experimental Methods

2.1 *Prediction of the membrane topology of Sec59p*

In order to predict the membrane topology of Sec59p, a WWW algorithm server, TOPCONS[20] (https://topcons.cbr.su.se) was used. On its WEB site, the amino acid sequence of Sec59p consisting of 519 residues was registered and surveyed regarding its potential transmembrane domains (TMDs) and membrane topology.

2.2 *Construction of recombinant plasmids for the YSUS*

The coding region of *SEC59* gene was amplified from genomic DNA derived from *Saccharomyces cerevisiae* NMY51 strain by standard PCR method[21] using SC59BPfw and SC59BPrv primers listed in Table 1. A PCR product was then digested with *Sfi* I, purified and ligated to the pBT-N or pBT-C plasmid vector for expression of Sec59p bait protein which has Cub (*C*-terminal half of ubiquitin protein) tag prepared in the YSUS, at the *N*- or *C*- terminus, respectively. Subsequently, the ligation mix was used for transformation of *Escherichia coli* JM109 strain prepared by SEM method[22]. Preparation of each recombinant plasmid from the transformants was conducted by standard cloning method[23], generating pBT-N-SC59 and pBT-C-SC59 bait constructs (Fig. 2).

In order to analyze membrane topology of Sec59p, thirteen pBT-C-based constructs (pBT-C-SC59/LR2 to pBT-

Table I The PCR primers used in this study. Additional sequences containing a *Sfi* I- cleavage site are shown in lowercase letters.

Primer name	Nucleotide sequence	Purpose
SC59BPfw	5'-tgtaatggccattacggccATGGTCGCTATAATACCTCATGCTTCC-3'	Cloning of full-length and truncated *SEC59*
SC59BPrv	5'- gcctttggccgaggcggccAGAGTAATTAATTTTTCACAAATCATCATAAAT-3'	Cloning of full-length *SEC59*
SC59(LR2)BPrv	5'- gcctttggccgaggcggccTTATAAGATATATCAGCGGTAACAATG-3'	Cloning of truncated *SEC59* from *N*-terminus to LR2
SC59(LR3)BPrv	5'- gcctttggccgaggcggccGTATCGAACTTGGGTAGGCTTTTG-3'	Cloning of truncated *SEC59* from *N*-terminus to LR3
SC59(LR4)BPrv	5'- gcctttggccgaggcggccCCATCTATATGAATTTAATACCGAAAG-3'	Cloning of truncated *SEC59* from *N*-terminus to LR4
SC59(LR5)BPrv	5'-gcctttggccgaggcggccTTCAATTGCCCAATATACTTCAAAATTA-3'	Cloning of truncated *SEC59* from *N*-terminus to LR5
SC59(LR6)BPrv	5'-gcctttggccgaggcggccACTGTGCCAGCCTCTGAAACGTA-3'	Cloning of truncated *SEC59* from *N*-terminus to LR6
SC59(LR7)BPrv	5'-gcctttggccgaggcggccTTAAAGTGCATTACCTTTTTGAGCAC-3'	Cloning of truncated *SEC59* from *N*-terminus to LR7
SC59(LR8)BPrv	5'-gcctttggccgaggcggccTGACGAATAGTAGACTCTAAGATATAT-3'	Cloning of truncated *SEC59* from *N*-terminus to LR8
SC59(LR9)BPrv	5'-gcctttggccgaggcggccTTTCGGGAGGTGTTCAACGATAGA-3'	Cloning of truncated *SEC59* from *N*-terminus to LR9
SC59(LR10)BPrv	5'-gcctttggccgaggcggcCAATGCAATTTTCACAAAGTTTGAATC-3'	Cloning of truncated *SEC59* from *N*-terminus to LR10
SC59(LR11)BPrv	5'-gcctttggccgaggcggcCCCGCTGTGGTCCCTATCATCA-3'	Cloning of truncated *SEC59* from *N*-terminus to LR11
SC59(LR12)BPrv	5'-gcctttggccgaggcggcCATTGGAGAGTTATTCATTAATAAAGG-3'	Cloning of truncated *SEC59* from *N*-terminus to LR12
SC59(LR13)BPrv	5'-gcctttggccgaggcggcCTCTAAAGTTTTTTGTGTACCTTTCC-3'	Cloning of truncated *SEC59* from *N*-terminus to LR13
SC59(LR14)BPrv	5'-gcctttggccgaggcggccAGGTGGTTAAAAATTGCAGCTTTATC-3'	Cloning of truncated *SEC59* from *N*-terminus to LR14

C-SC59/LR14) for expression of the *C*-terminally truncated Sec69p bait proteins in yeast were prepared via PCR cloning described above (Fig. 2).

In order to analyze the physical interaction of Sec59p, the prey constructs (pPR-N-SC59 and pPR-C-SC59) that would express Sec59p prey protein having Nub G (*N*-terminal half of I13G mutational ubiquitin protein) tag at the *N*- or *C*- terminus, were also prepared by the same procedure, except usage of the pPR-N and pPR-C plasmid vectors instead of the pBT-N and pBT-C vectors, respectively (Fig. 2).

2.3 *Assays for the membrane topology of Sec59p*

The bait constructs (the pBT-N-SC59, pBT-C-SC59 and thirteen pBT-C-hSC59/LR series) were used for co-transformation of yeast NMY51 strain, together with the negative control prey construct (pDL-Alg5) or positive control prey construct (pAI-Alg5). The transformation of the yeast cells was carried out by the standard method[24].

The co-transformants obtained on the synthetic dextrose (SD) medium lacking leucine and tryptophan (SD-LW) were then subject to the growth examination on the SD medium lacking leucine, tryptophan and histidine (SD-LWH) and SD medium lacking leucine, tryptophan, histidine and adenine (SD-LWHA) according to the manual supplied by Dualsystems Biotech (www.dualsystems.com).

2.4 *Assays for the physical interaction of hDK*

The bait construct, pBT-N-SC59 or pBT-C-SC59, was combined with the prey construct, pPR-N-SC59 or pPR-C-SC59, and then they were used for co-transformation of yeast NMY51 strain. After the co-transformation, the co-transformants grown on SD-LW medium were subject to growth examination with SD-LWH and SD-LWHA media, according to the same procedure as described above.

3. Results and Discussion

3.1 *The membrane topology of Sec59p*

The Sec59p protein is composed of 519 amino acid residues[3]. First, we started from predicting the membrane topology of Sec59p with TOPCONS algorithm[20], a server freely available on WEB sites. It consists of five independent algorithms (SCAMPI-seq, SCAMPI-msa, PRODIV, PRO and OCTOPUS in Fig. 1) that predict TMDs and membrane topology of a protein. Based on five predictions derived from their algorithms, TOPCONS concludes one consensus prediction. As shown in Fig. 1, TOPCONS consequently predicted fifteen loop regions (LRs 1 to 15) and fourteen hydrophobic regions (HRs 1 to 14) corresponding to potential TMDs in Sec59p. It also predicted that both *N*- and *C*-termini would be orientated toward cytoplasmic sides of the rER membrane.

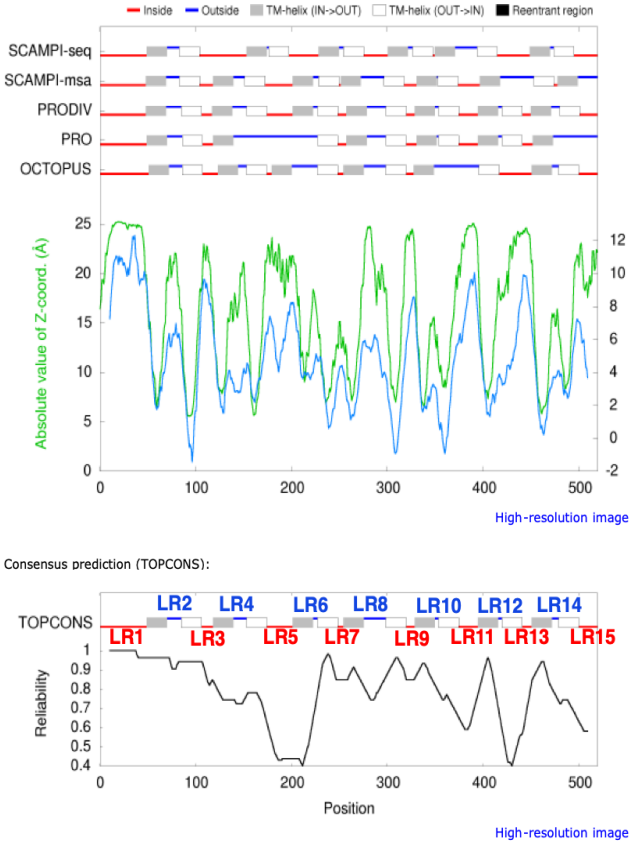

Fig. 1 Prediction of the membrane topology of Sec59p by TOPCONS algorithm server (http://topcons.cbr.su.se/). The fourteen hydrophobic regions (HR1 to HR14) are indicated with boxes, as candidates of transmembrane domains (TMDs), and the fifteen loop regions (LR1 to LR15) are indicated with red or blue lines, as cytoplasmic or luminal loops, respectively.

In order to examine this prediction, we applied the YSUS to our analysis of Sec59p. The YSUS prepares two prey constructs (pDL-Alg5 and pAI-Alg5) as negative and positive control, respectively. pAI-Alg5 is designed to express Nub I (*N*-terminal half of ubiquitin protein) tag *C*-terminally fused to Alg5p protein on the cytoplasmic side of the rER, and readily available to judge whether the terminal Cub tag fused to the bait protein expressed on the rER membrane is located in the cytoplasm or lumen[13-19]. Firstly, we prepared the two bait constructs, pBT-N-SC59 and pBT-C-SC59, which express a full-length Sec59p protein with *N*- and *C*-terminal Cub tags, respectively (Fig. 2). Each bait construct was combined with the pDL-Alg5 or pAI-Alg5 control prey, and then they were used for co-transformation of yeast NMY51 cells. As shown in Fig. 3, co-transformants of pDL-Alg5 or pAI-Alg5 with pDL-Alg5 did not grow on the two selective media (SD-LWH and SD-WWHA), but those with pAI-Alg5 grew on them (top red frame and bottom red frame). These results indicated that both termini of Sec59p were located in the cytosol (Fig. 5). Next, we prepared thirteen additional bait constructs, pBT-C-SC59/LR2 to pBT-C-SC59/LR14, each of which would express truncated Sec59p protein, which has Cub tag at *C*-terminus (Fig. 2) and conducted similar growth examination. As a

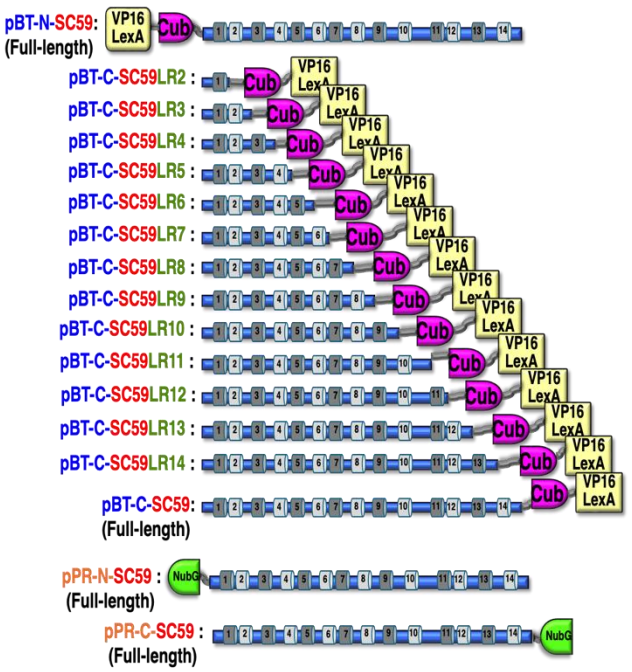

Fig. 2 Plasmid constructs and expressed proteins in this study. Bars and boxes of proteins indicate loop regions (LRs) and hydrophobic regions (HRs), respectively.

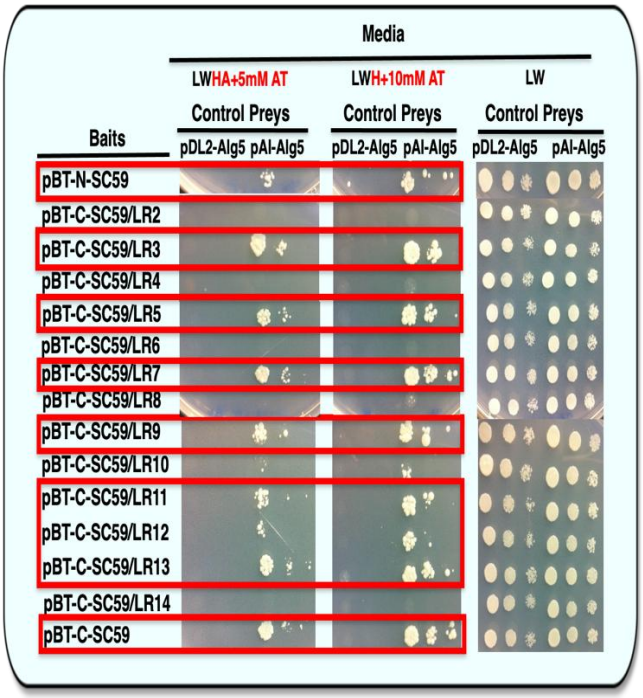

Fig. 3 Growth examination of co-transformants using two full-length Sec59p baits and thirteen truncated Sec59p baits. After the selection of colonies derived from the co-transformants on the SD-LW medium, their suspensions were diluted with sterilized water and adjusted to the OD_{600} values of 1.0, 0.1 and 0.01 (from left to right). These diluents were orderly spotted on the SD-LWH and SD-LWHA media for reporter detection, and SD-LW media for growth control, and then incubated at 30 ºC for 2~4 days. 3-amino-triazole (AT) was added to SD-LWH and SD-LWHA media at concentration of 10 and 5 mM respectively, for preventing background growth due to leaky *HIS3* gene expression.

result, co-transformants of pBT-C-SC59/LR3, pBT-C-SC59/LR5, pBT-C-SC59/LR7, pBT-C-SC59/LR9, pBT-C-SC59/LR11, pBT-C-SC59/LR12 and pBT-C-SC59/LR13 with pAI-Alg5 displayed viability on two selective media (red frames in Fig. 3). These observations suggested that the LR3, LR5, LR7, LR9, LR11, LR12 and LR13 of Sec59p might be located in the cytoplasmic side of the rER membrane (Fig. 5). In contrast, co-transformants of pBT-C-SC59/LR2, pBT-C-SC59/LR4, pBT-C-SC59/LR6, pBT-C-SC59/LR8, pBT-C-SC59/LR10 and pBT-C-SC59/LR14 did not grow on two selective media (Fig. 3). These observations suggested that the LR2, LR4, LR6, LR8, LR10 and LR14 of Sec59p might be located in the luminal side of the rER membrane (Fig. 5).

Taken together, our membrane topological analysis of Sec59p demonstrated that it has at least twelve TMDs with *N*- and *C*- termini oriented towards cytosol, as a topological model proposed in Fig. 5. This model differs from that predicted in Fig. 2, with regard to the number of TMD. Although the possibility that the HR11 and HR12 of Sec59p would be potential membrane-embedded domains cannot be excluded, our model is so far the only one which were exhibited based on the experimental evidence.

Sec59p possesses a KTxEG motif, which might bind CTP or be a putative catalytic domain[4], around the LR13 (a violet frame in Fig. 5). Therefore, the LR13 must be located within the cytoplasm, because CTP is biosynthesized in the cytoplasm. Hence, our model is suitable for this fact.

3.2 *The self-interaction of Sec59p*

In order to test whether Sec59p physically interacts with itself, each of the two bait constructs pBT-N-SC59 and pBT-C-SC59, was combined with each of the two prey constructs, pPR-N-SC59 and pPR-C-SC59, and then transformation of the NMY51 cells were conducted. In growth examination shown in Fig. 4A, co-transformants of pBT-N-SC59 and pPR-N-SC59 could grow on SD-LWH and SD-LWHA media (an upper red frame in Fig. 4A), but those of pBT-N-SC59 and pPR-C-SC59 could not. These results indicate that *N*-terminus of Sec59p bait would be proximal to *N*-terminus of Sec59p prey, but distal to *C*-terminus of Sec59p prey probably due to conformational reason.

On the other hand, co-transformants with pBT-C-SC59 and pPR-N-SC59/pPR-C-SC59 could grow on the selective media (a red frame in Fig. 4B), suggesting that *C*-terminus of Sec59p bait would be accessible to both termini of Sec59p prey. Interestingly, co-transformants of pBT-C-SC59 and pPR-C-SC59 apparently grew on the selective media better than those of pBT-C-SC59 and pPR-N-SC59 (a red frame in Fig. 4B), indicating that *C*-terminus of Sec59p prey, rather than *N*-terminus of Sec59p prey, preferentially interacts with *C*-terminus of Sec59p bait. This fact might reflect the three-dimensional arrangement of two Sec59p proteins in homodimer formed on the rER membrane.

4. Conclusion

In order to determine the membrane topology of yeast Sec59p which *de novo* produces the Dol-P required for the assembly of DLOs, the YSUS was utilized. Results obtained

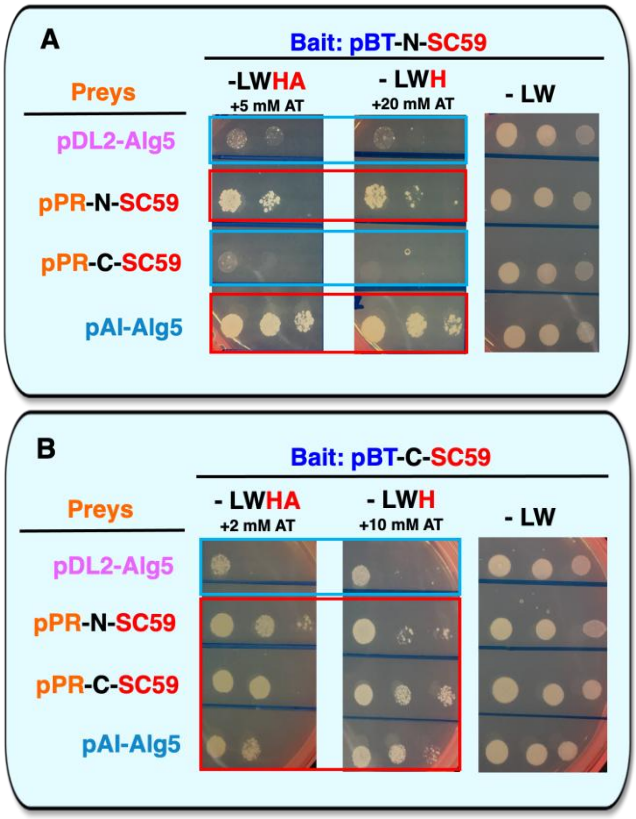

Fig. 4 (A) Growth examination of co-transformants of pBT-N-SC59 with pPR-N-SC59 or pPR-C-SC59. (B) Growth examination of co-transformants of pBT-C-SC59 with pPR-N-SC59 or pPR-C-SC59. The experiments were carried out according to the same procedure as described in the legend of Fig. 3, except usage of LWH medium containing 20 mM AT in (A) and LWHA medium containing 2 mM AT in (B).

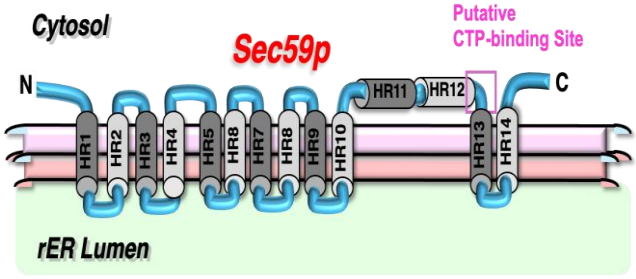

Fig. 5 The model of membrane topology of Sec59p based on the YSUS analyses indicated in Fig. 3. Putative catalytic site is indicated by a violet frame.

from analyses by the YSUS demonstrated that Sec59p protein contains at least twelve TMDs, with both *N*- and *C*-termini located in the cytoplasmic side of the rER membrane (Fig. 3 and Fig. 5).

With respect to the physical interactions of Sec59p, we obtained a novel information strongly suggesting that it might homodimerize on the rER membrane (Fig. 4). It is possible to identify a region required for this self-interaction, by using a series of bait constructs for expression of truncated Sec59p baits, which we prepared in this study. In addition. we are now preparing a series of prey constructs for expression of truncated Sec59p preys in order to explore the interacting region.

The physical interaction between two membrane enzymes could play a role in positively or negatively altering their enzymatic activities. In this study, we found out that Sec59p forms at least homo-dimeric complex on the rER membrane. This fact raises the possibility that DK activity might be regulated by the status of homo-oligomerization of Sec59p at protein level. On the other hand, we recently demonstrated that Alg5p bait, which is yeast DPGS, physically interacts with Sec59p prey in another YSUS analysis[14]. This observation means that Sec59p might also form hetero-dimeric complex on the rER membrane. Hence, we are now investigating the physical interactions of Sec59p bait with preys of other enzymes involved in DLO assembly.

References

1) M. Aebi, *N*-linked protein glycosylation in the ER, Biochim. Biophys. Acta Vol.1833, pp.2430-2437 (2013).
2) M. Bernstein, F. Kepes and R. Schekman, *SEC59* encodes a membrane protein required for core glycosylation in *Saccharomyces cerevisiae*, Mol. Cell. Biol. Vol.9, pp.1191-1199 (1989).
3) L. Heller, P. Orlean and W. L. Adair Jr., *Saccharomyces cerevisiae* sec59 cells are deficient in dolichol kinase activity, Proc. Natl. Acad. Sci. USA Vol.89, pp.7013-7016 (1992).
4) F. Fernandez, P. Shridas, S. Jiang, M. Aebi, C. J. Waechter, Expression and characterization of a human cDNA that complements the temperature-sensitive defect in dolichol kinase activity in the yeast *sec59-1* mutant: the enzymatic phosphorylation of dolichol and diacylglycerol are catalyzed by separate CTP-mediated kinase activities in *Saccharomyces cerevisiae*. Glycobiology Vol.12, pp.555–562 (2002).
5) N. Johnsson and A. Varshavsky, Split ubiquitin as a sensor of protein interactions *in vivo*, Proc. Natl. Acad. Sci. USA Vol.91, No.22, pp.10340-10344 (1994).
6) I. Stagljar, C. Korostensky, N. Johnsson and S. te Heesen, A genetic system based on split-ubiquitin for the analysis of interactions between membrane proteins *in vivo*, Proc. Natl. Acad. Sci. USA Vol.95, pp.5187-5192 (1998).
7) M. Fetchko and I. Stagljar, Application of the split-ubiquitin membrane yeast two-hybrid system to investigate membrane protein interactions, Methods Vol.32, pp.349-362 (2004).
8) S. Thaminy, J. Miller and I. Stagljar, The split-ubiquitin membrane-based yeast two-hybrid system, Methods. Mol. Biol. Vol.261, pp.297–312 (2004).
9) M. Dünnwald, A. Varshavsky and N. Johnsson, Detection of transient *in vivo* interaction between substrate and transporter during protein translocation into the endoplasmic reticulum, Mol. Biol. Cell Vol.10, pp.329-344 (1999).
10) M. J. Massaad and A. Herscovics, Interaction of the endoplasmic reticulum alpha 1, 2-mannosidase Mns1p with Rer1p using the split-ubiquitin system, J, Cell Sci. Vol.114, pp.4629-4635 (2001).
11) W. Scheper, S. Thaminy, S. Kais, I. Stagljar and K. Römisch, Coordination of *N*-glycosylation and protein translocation across the endoplasmic reticulum membrane by Sss1 protein, J. Biol. Chem. Vol.278, No.39, pp.37998-38003 (2003).
12) A. Yan and W. J. Lennarz, Studies on yeast oligosaccharyl transferase subunits using the split-ubiquitin system: Topological features and *in vivo* interactions, Proc. Natl. Acad. Sci. USA Vol.102, No.20, pp.7121-7126 (2005).
13) T. Takahashi and T. Takeuchi, Membrane topological characterization of the human Alg14 protein, Proc. Schl. Eng. Tokai Univ., Ser. E Vol.44, pp.1-6 (2019).
14) Samantha and T. Takahashi, Analyses of the membrane topology and physical interaction of dolichyl-phosphate-glucose synthase Alg5p, Proc. Schl. Eng. Tokai Univ., Ser. E Vol.49, pp.19-25 (2024).
15) T. Takahashi and X. -D. Gao, Physical interactions among human glycosyltransferases involved in dolichol-linked oligosaccharide biosynthesis, Trends in Glycoscience and Glycotechnology Vol.24, No.136, pp.65-77 (2012).
16) T. Takahashi, N. Yamada and N. Kurimoto, Analyses on the physical interactions of the human dolichyl-phosphate-mannose synthase, Proc. Schl. Eng. Tokai Univ., Ser. J. Vol.57, No.1, pp.5-10 (2017).
17) T. Takahashi, K. Nishimura, N. Maeda and R. Oshiro, Characterization of the membrane topology and physical interaction of human *N*-acetylglucosamine-1-phosphate transferase, Proc. Schl. Eng. Tokai Univ., Ser. E Vol.46, pp.1-6 (2021).
18) T. Takahashi, N. Yamada and R. Oshiro, Characterization of the membrane topology and physical interaction of human dolichol-phosphate-glucose synthase, Proc. Schl. Eng. Tokai Univ., Ser. E Vol.47, pp.1-6 (2022).
19) T. Takahashi, E. Horigome, T. Yamanoto and K. Terajima, Analyses of the membrane topology and physical interaction of human dolichol kinase, Proc. Schl. Eng. Tokai Univ., Ser. E Vol.49, pp.13-18 (2024).
20) K. D. Tsirigos, C. Peters, N. Shu, L. Käll and A. Elofsson, The TOPCONS web server for consensus prediction of membrane protein topology and signal peptides, Nucleic Acids Res. 43(Web Server issue) W401-407 (2005).
21) H. A. Erlich, PCR Technology, Stockton Press, pp.61-70 (1989).
22) H. Inoue, H. Nojima and H. Okayama, High efficiency transformation of *Escherichia coli* with plasmids, Gene Vol. 96, pp.23–28 (1990).
23) L. Sambrook, E. F. Fritsch and T. Maniatis, Molecular Cloning: A Laboratory Manual. Second edition, Cold Spring Harbor Laboratory Press, NY, (1989).
24) H. Ito, Y. Fukuda, K. Murata and A. Kimura, Transformation of intact yeast cells treated with alkali cations, J. Bacteriol. Vol.153, No.1, pp.163-168 (1983).

The School of Engineering of Tokai University publishes two kinds of Reports: the report written in English (once a year) and the one written in Japanese (once a year).

*　　*　　*

Any requests for this proceedings should be addressed to the Editorial Committee of Proceedings of the School of Engineering Tokai University, 4-1-1, Kitakaname, Hiratsuka-shi, Kanagawa-ken. Japan

September 30, 2025

Attention:

The name of this PROCEEDINGS has been changed from 2018 edition as follows.

「PROCEEDINGS OF *THE SCHOOL OF ENGINEERINGS*」